MODELING OF A SHAPE MEMORY ALLOY POSITION CONTROL SYSTEM AND L2 STABILITY ANALYSIS

NORHALIZA BT. HJ. ABDUL WAHAB
PM YAHYA MD SAM
PM DR FUAAD B RAHMAT

UNIVERSITI TEKNOLOGI MALAYSIA

VOT 71950

MODELING OF A SHAPE MEMORY ALLOY POSITION CONTROL SYSTEM AND L2 STABILITY ANALYSIS

(MEREKABENTUK SISTEM KAWALAN KEDUDUKAN BAGI ALOI INGATAN BENTUK DAN ANALISIS KESTABILAN L2)

NORHALIZA BT. HJ. ABDUL WAHAB
PM YAHYA MD SAM
PM DR FUAAD B RAHMAT

FAKULTI KEJURUTERAAN ELEKTRIK
UNIVERSITI TEKNOLOGI MALAYSIA

2004

Lampiran 20

UTM/RMC/F/0024 (1998)

UNIVERSITI TEKNOLOGI MALAYSIA

BORANG PENGESAHAN
LAPORAN AKHIR PENYELIDIKAN

TAJUK PROJEK : MODELING OF A SHAPE MEMORY ALLOY POSITION CONTROL SYSTEM AND L2 STABILITY ANALYSIS.

Saya NORHALIZA BT HJ ABDUL WAHAB
(HURUF BESAR)

Mengaku membenarkan **Laporan Akhir Penyelidikan** ini disimpan di Perpustakaan Universiti Teknologi Malaysia dengan syarat-syarat kegunaan seperti berikut :

1. Laporan Akhir Penyelidikan ini adalah hakmilik Universiti Teknologi Malaysia.
2. Perpustakaan Universiti Teknologi Malaysia dibenarkan membuat salinan untuk tujuan rujukan sahaja.
3. Perpustakaan dibenarkan membuat penjualan salinan Laporan Akhir Penyelidikan ini bagi kategori TIDAK TERHAD.
4. * Sila tandakan (/)

☐	SULIT	(Mengandungi maklumat yang berdarjah keselamatan atau Kepentingan Malaysia seperti yang termaktub di dalam AKTA RAHSIA RASMI 1972).
☐	TERHAD	(Mengandungi maklumat TERHAD yang telah ditentukan oleh Organisasi/badan di mana penyelidikan dijalankan).
☐	TIDAK TERHAD	

TANDATANGAN KETUA PENYELIDIK

Nama & Cop Ketua Penyelidik

Tarikh : 25 MAC 2004

NORHALIZA ABDUL WAHAB
Pensyarah
Jab. Kawalan Dan Instrumentasi
Fakulti Kejuteraan Elektrik
Universiti Teknologi Malaysia
Skudai, Johor Darul Takzim
Email : aliza@suria.fke.utm.my
Tel : 07-5505065

CATATAN : ** Jika Laporan Akhir Penyelidikan ini SULIT atau TERHAD, sila lampirkan surat daripada pihak berkuasa/ organisasi berkenaan dengan menyatakan sekali sebab dan tempoh laporan ini perlu dikelaskan sebagai SULIT dan TERHAD.*

ACKNOWLEDGEMENT

First and foremost, I wish to express my deepest gratitude to my colleague PM Yahaya Md Sam and PM Dr Fuaad Rahmat for an invaluable cooperation in order to finish this project.

I would like to thank all my friends and research students who have help and support me in accomplishing this project.

ABSTRACT

Simple, light, and powerful, shape memory actuators hold much promise for the future of development technology of engineering. Since the discovery of shape memory in nickel-titanium, a number of inventions have been made having applications in medicine, aerospace, automotive, and consumer products. In this thesis, a discussions about the application of shape memory alloys (SMA) and shape memory effect to actuators will be explained more detail and specified. Conventional actuators also elaborated for gives early approach to understanding the operations of actuator in engineering. A simple shape memory alloy-actuated position control system was developed by an experimental system using a single SMA wire actuator, under constant load. The dissipativity-related stability was applied to an experimental. It is shown that, for a broad class of dissipativity controllers, the system will be L2 stable for some range of non-zero loop gain. This applies to the common P, PI, PD, and PID controllers, among others, and believe to be the first result of its kind. During the experimental, three different parameters have been achieved and simulation result will be shows for approach of stability system. It is shown that, interesting non-linear dynamic characteristics of the SMA actuator.

ABSTRAK

Mudah, kecil dan berkuasa, penggerak (actuator)aloi ingatan bentuk menjanjikan masa depan kepada perkembangan teknologi kejuruteraan. Sejak penemuan aloi ingatan terhadap nikel-titanium, banyak rekacipta dilakukan dalam aplikasi seperti perubatan, ruang angkasa, automotif dan produk pengguna. Dalam tesis ini, perbincangan tentang aplikasi aloi ingatan bentuk dan kesan aloi ingatan terhadap penggerak akan diterangkan dengan lebih terperinci dan khusus. Penggerak konvensional juga dihuraikan untuk memberikan pengenalan dan pendekatan awal kepada kefahaman operasi sebuah penggerak dalam kejuruteraan. Satu penggerak aloi ingatan yang mudah dalam sistem kawalan kedudukan akan dikembangkan melalui eksperimen menggunakan satu wayar SMA penggerak, dengan beban yang tetap. Rajah blok yang berhubung dengan kestabilan diaplikasikan kepada eksperimen yang dijalankan. Ia menunjukkan untuk jenis pengawal yang liberal, sistem akan memberikan L2 stabil untuk beberapa julat pekali gelung bukan sifar. Pengawal yang digunakan adalah pengawal P, PI, PD dan PID dan yakin ia adalah keputusan pertama bagi jenis pengawal tersebut. Melalui eksperimen, tiga parameter berbeza akan diperolehi dan keputusan simulasi dilihat untuk pendekatan kestabilan sistem. Ia akan menunjukkan ciri-ciri dinamik tak linear yang menarik untuk penggerak SMA.

CONTENTS

LIST OF TABLE

LIST OF FIGURE

LIST OF SYMBOL

SMA	-	Shape memory alloy
NiTi	-	Nickel titanium
A_s	-	Austenite start temperature
A_f	-	Austenite finish temperature
M_s	-	Martensite start temperature
M_f	-	Martensite finish temperature
M_d	-	Highest temperature to strain-induced martensite
σ_M	-	Stress at the martensite phase
ε_M	-	Strain at the martensite phase
I	-	Current
V	-	Voltage drop
R	-	Resistance
P	-	Power
σ_h	-	Tensile stress in austenite condition
ε_h	-	Strain in austenite condition
σ_l	-	Tensile stress in martensite condition
ε_l	-	Strain in martensite condition
d	-	Diamater
F	-	Force
L	-	wire length
V_m	-	Input voltage
I_L	-	Current load

LIST OF APPENDICES

CHAPTER 1

INTRODUCTION

1.1 Background

The first Shape Memory Alloys (SMA) appeared about 50 years ago, and gained momentum with the discovery at the Naval Ordnance Laboratory in the 1960s of nickel-titanium SMA. These were named Ni-Ti-NOL, and the name still applies to these materials. The more common abbreviation is NiTi. Many other SMA have been developed. This discussion research is limited to nickel-titanium based systems.

Actuators do not constitute the largest amounts of NiTi in use. These are superelastic devices, in antennas for cellular telephones, in eyeglass frames and in medical devices, especially catheter guide wires, dental arches, and stents. Herewith is a brief review of selected examples of shape-memory actuators. This is not a recitation of all the devices made but an attempt to recall some historical machines, look at some of the current uses, and suggest where this industry might go in the not-too-distant future.

The reason for use of shape-memory alloys as actuators is that a large amount of work can be obtained in a small volume. As a result, many newer actuators have been developed, which respond to the criteria for reduced size. One of the more promising outcome of this research has been the application of shape memory alloys (SMA) and shape memory effect to actuators.

1.2 Project Objective

The main objective of this project is to understanding the actuators development in the several industrial especially shape memory alloys actuators.

Secondly, the objective of this project is to understanding the theory and general behavior of shape memory alloys elements. They are used in actuators application and commercial aspect.

The next objective is to identify the characteristic of design shape memory alloy actuators.

This project is also developed for position control using a single SMA wire actuators, under constant load. The experimental setup as elaborated in chapter 6.

1.3 Scope of The Project

This project involves hardware design and development the design of shape memory alloys wire actuators based on simple experimental system for position control, under constant load. The hardware is using an electric current to be heated the SMA element. While control current is driven through the SMA by a voltage-to-current converter. The load of 2 kg is chosen such that the SMA wire is stretched. Three different parameters were experimentally measured during the experiments: SMA wire voltage drop, SMA wire current, and SMA wire contraction. These tests showed interesting non-linear dynamic characteristics of the actuator. Beside that, the dissipativity-related stability was applied to an experimental. This applies to the common P, PI, PD, and PID controllers, among others, and believe to be the first result of its kind . An important observation made during the dynamic analysis was the unpredictability of the actuator's response when low to moderate voltages are applied. This characteristic strongly suggests chaotic behavior of the actuator, which could potentially cause control difficulties in fine and high accuracy tasks.

1.4 Overview

This thesis was written to bring the readers step by step going into the main part of the content. It is divided into 7 chapters and each chapter will be briefly discussed in this section.

Chapter 2 describes the shape memory alloys used in this project. It gives a complete foundation of shape memory alloys and the general behavior of shape memory

alloys effect. This is important to understand the development of the shape memory elements.

Chapter 3 discusses the conventional actuators. This chapter explains the three main type of actuations have been the core of motion and force power for all robotic systems. They are Hydraulic, Pneumatic, and Electric motors.

Chapter 4 concerns about the shape memory alloys actuators. This chapter also discuss about the shape memory alloys actuators in robotic and commercial applications. Advantages and drawbacks in use of SMA actuation mechanism also are elaborated.

Chapter 5 elaborates the design of wire SMA actuators. It mainly explains design method of shape memory wire. Then, the experimental ystem has been developed for position control using a single SMA wire actuator, under constant load discusses in Chapter 6. The result of this system is presented also in that chapter.

This thesis ends up with Chapter 7 to give an overall conclusion for the project. This chapter also discusses some suggestions and ideas for the future development of this project.

CHAPTER 2

THEORY AND GENERAL BEHAVIOR OF SMA

This chapter provides the theory and general behavior required to form an understanding of shape memory alloys and the shape memory effect.

2.1 Shape Memory Alloys

This section describes the theory required to understand what are shape memory alloys and the operation of shape memory alloys. Shape memory alloys (SMA) are metals, which exhibit two very unique properties, pseudo-elasticity, and the shape memory effect. Arne Olander first observed these unusual properties in 1938, but not until the 1960's were any serious research advances made in the field of shape memory alloys. The most effective and widely used alloys include NiTi (Nickel - Titanium), CuZnAl, and CuAlNi.

Many different metal alloys have been found to display shape memory alloy properties. The most commonly used in electrical actuator application is a near-binary mixture of nickel and titanium, called NiTi since it was first developed at the US Naval Ordinance Laboratory. NiTi shape memory metal alloy can exist in a two different temperature-dependent crystal structures (phases) called martensite (lower temperature) and austenite (higher temperature or parent phase). Several properties of austenite NiTi and martensite NiTi are notably different.

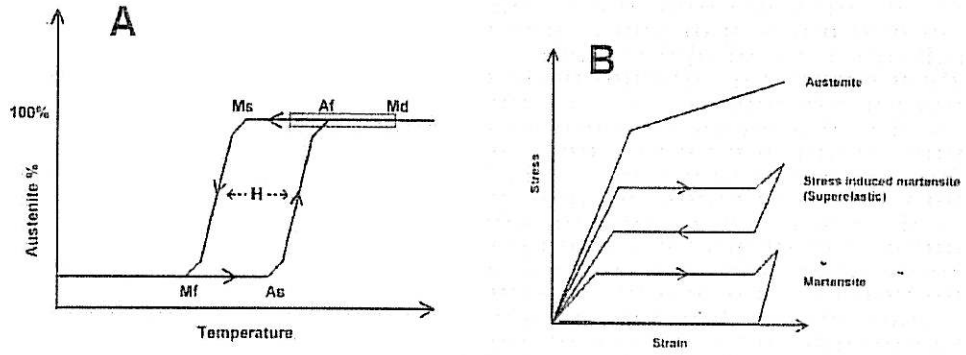

Figure 2.1 Austenite-temperature and Stress-strain behavior

(A) Martensitic transformation and hysteresis (= H) upon a change of temperature. As = austenite start, Af = austenite finish, Ms = martensite start, Mf = martensite finish and Md = Highest temperature to strain-induced martensite. Gray area = area of optimal superelasticity. B) Stress-strain behavior of different phases of NiTi at constant temperature.

When martensite NiTi is heated, it begins to change into austenite (Figure 2.1 A). The temperature at which this phenomenon starts is called austenite start temperature

(A_s). The temperature at which this phenomenon is complete is called austenite finish temperature (A_f). When austenite NiTi is cooled, it begins to change into martensite. The temperature at which this phenomenon starts is called martensite start temperature (M_s). The temperature at which martensite is again completely reverted is called martensite finish temperature (M_f).

Composition and metallurgical treatments have dramatic impacts on the above transition temperatures. From the point of view of practical applications, NiTi can have three different forms: martensite, stress-induced martensite (superelastic), and austenite. When the material is in its martensite form, it is soft and ductile and can be easily deformed (somewhat like soft pewter). Superelastic NiTi is highly elastic (rubber-like), while austenitic NiTi is quite strong and hard (similar to titanium) (Figure 2.1 B). The NiTi material has all these properties, their specific expression depending on the temperature in which it is used. For a more complete description of the shape memory alloy effect and shape memory alloy fabrication and application, the reader is encouraged to consult this excellent source.

2.2 Shape Memory Effect

This section looks at shape memory effect, where the shape memory alloys possess the ability to undergo shape change at low temperature and retain this deformation until they are heated, at which point they return to their original shape. This shape change occurs as the result of a change in the atomic crystal structure of the alloy.

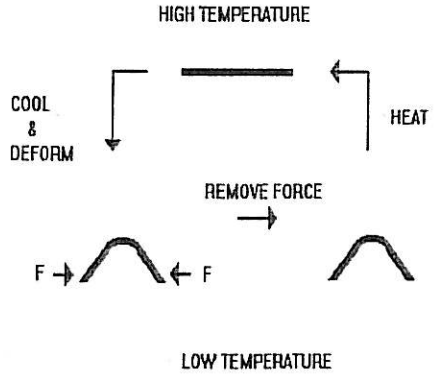

Figure 2.2 Bending of a shape memory wire

Using nickel-titanium (NiTi), the high temperature crystal structure, called is austenite (Figure 2.3 (a)). Upon cooling, the material transforms to a structure called martensite, with a monoclinic lattice structure which looks a parallelogram in two dimensions (Figure 2.3 (b)).

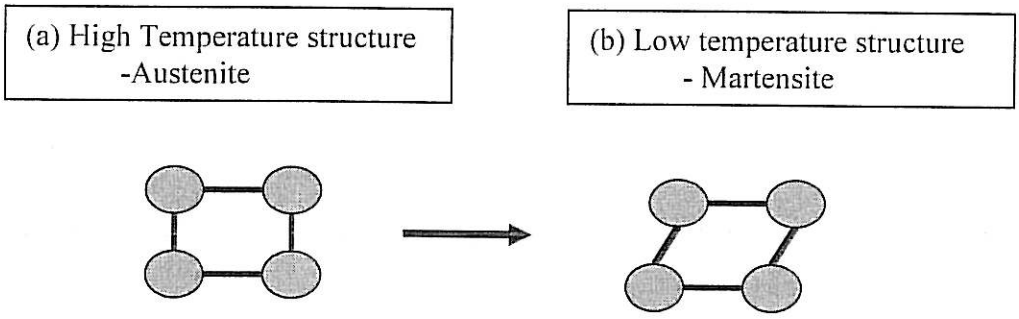

Figure 2.3 Nickel titanium shape memory alloy structure

However, when a piece of shape memory material containing many atoms is cooled, the atoms do not all tilt in the same direction, as one might expect. Alternating

rows of atoms tilting either left or right are formed. Note that any 4 connected atoms in the low temperature structure of figure 2.4 (b) .

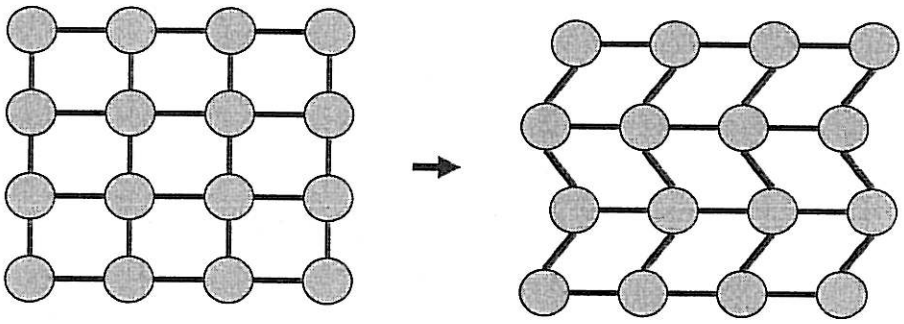

(a) High Temperature (b) Low Temperature

Figure 2.4 shape memory alloy atomic rearrangement upon cooling

This phenomenon is called twinning, because the atoms form mirror images of themselves, or twins, through a plane of symmetry (figure 2.5).

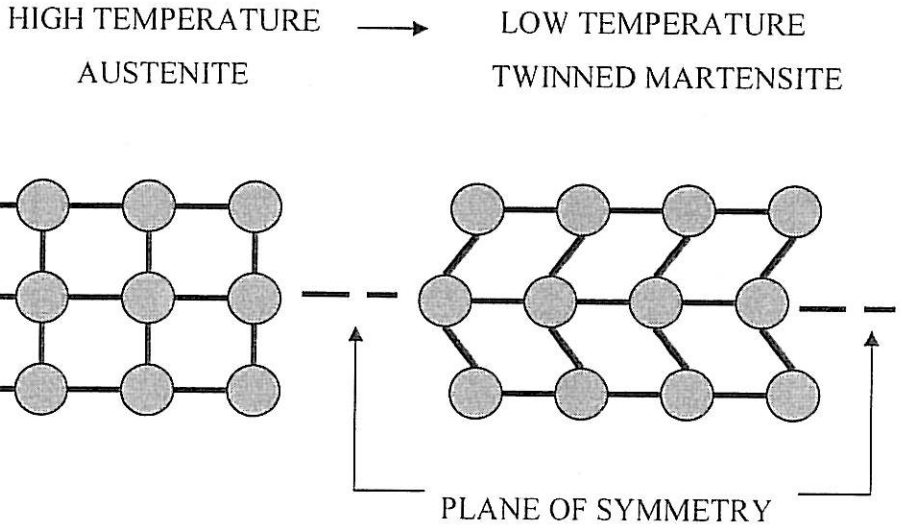

Figure 2.5 Twinning Mechanism

The twinned lattice structure occupies the same volume as the original structure, but because of the twinned nature of the lattice, it has a much lower Young's Modulus. When heated again, the alloy returns to the austenite phase, and the lattice recover its form.

The shape memory effect is visible only if the alloys is deformed while some martensite is present, and then reheated. When a stress is applied to the alloy it will deform as the twins are reoriented so they all lie in the same direction. This process is called "detwinned" (Figure 2.6). In shape memory alloys the stress require to reorient twins is relatively low. If the alloy is then heated, the deformed martensite will revert to austenite and the original shape of the piece will be obtained. This happen because the original atomic positions always maintained in the austenite phase.

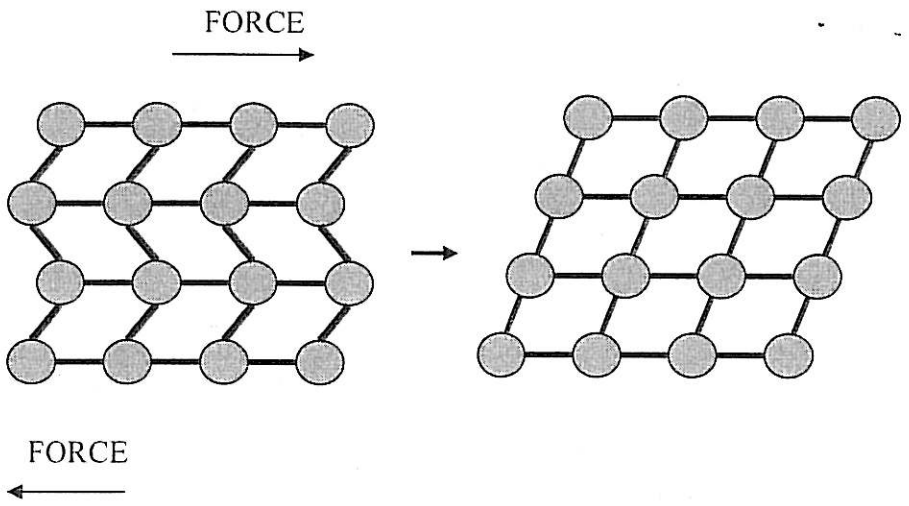

(a) As cooled (b) Deformed by applied force

Figure 2.6 Deformation of low temperature structure by applied force

Figure 2.7 shown the all structure of the shape memory alloy when heating and cooling applied to shape memory.

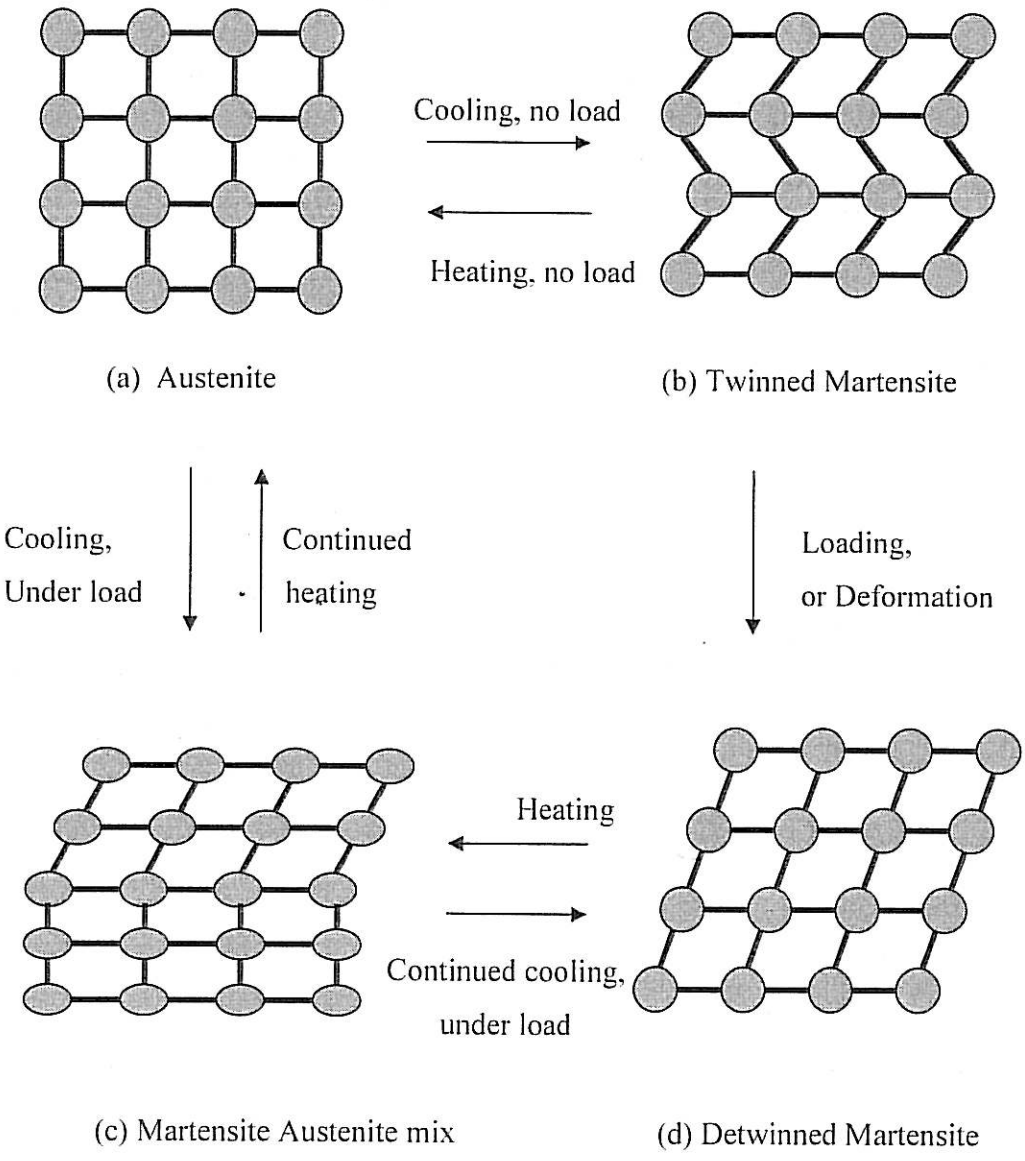

Figure 2.7 Lattice structures in Austenite and Martensite

2.2.1 Hysteresis

The temperature range for the martensite-to-austenite transformation, which takes place upon heating is somewhat higher than that for the reverse transformation upon cooling. The difference between the transition temperatures upon heating and cooling is called hysteresis. Hysteresis is generally defined as the difference between the temperatures at which the material is 50 % transformed to austenite upon heating and 50 % transformed to martensite upon cooling. This difference can be up to 20-30 °C.

2.3 Stress-Strain Behavior

The effect of different manufacturing and training technique on the performance of SMA is an active area of research in material science. Unlike conventional materials such as steel and aluminum which show only a limited effect of temperature on stress-strain behavior, shape memory alloys show a very marked temperature dependence, because of the reversible austenite-to-martensite transformation. The stress-strain characteristics behavior of a shape memory alloy at or below the M_f temperature are shown in Figure 2.8 . The microstructure consists of randomly oriented martensite twins (it is assumed that the material cooled from the austenite with no applied stress).

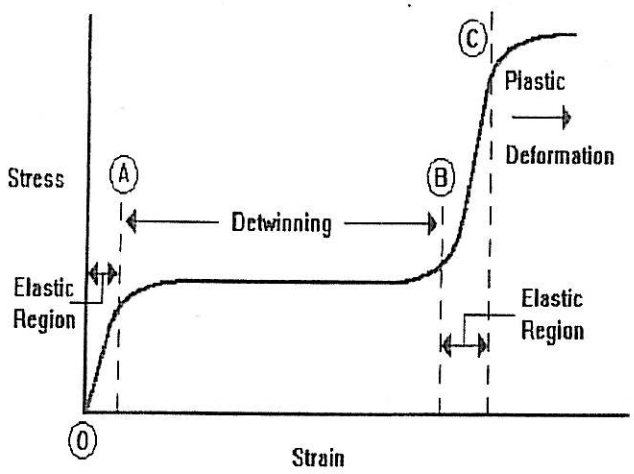

Figure 2.8 Shape Memory Alloys Stress-Strain Behavior at or below the M_f Temperature.

Thus in Figure 2.8 , the initial curve segment OA represents elastic deformation, until the stress level is sufficient to start the twins to reorient according to the applied stress field, at point A. In the segment AB the twins reorient until they all lie in the same crystalline structure – this process in known as "detwinng". Detwinning is complete at point B, and the martensite undergoes mostly elastic deformation again in segment BC. At point C the stress level is sufficient to start plastic deformation of the martensite.

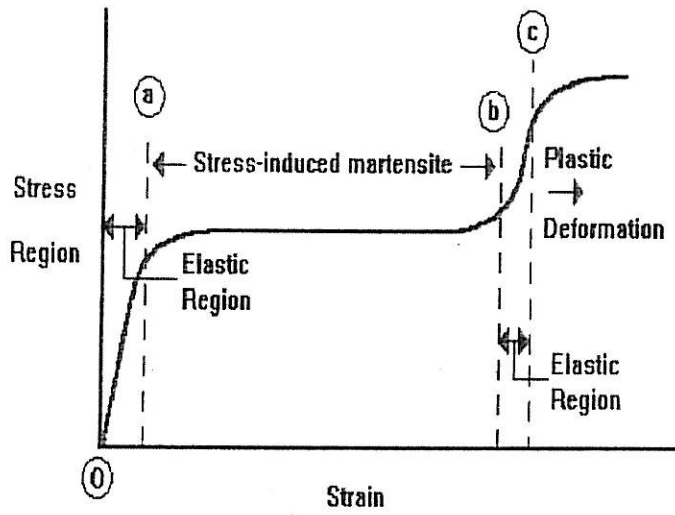

Figure 2.9 Stress-Strain Behavior above A_f and below M_d

Figure 2.9 shows the stress-strain behavior of a shape memory alloy at a temperature above A_f, and below the M_d temperature. Again the initial curve segment up to point "a" represent only elastic deformation. Martensite begins to form from the austenite ("a"). Then, in the curve segment ab the austenite is converted to martensite. Segment bc represents elastic deformation, with plastic deformation accruing after point "c" same as before in the Figure 2.7 . When the Figure 2.8 and Figure 2.9 to combined the two curve will be represented as shown in Figure 2.10 .

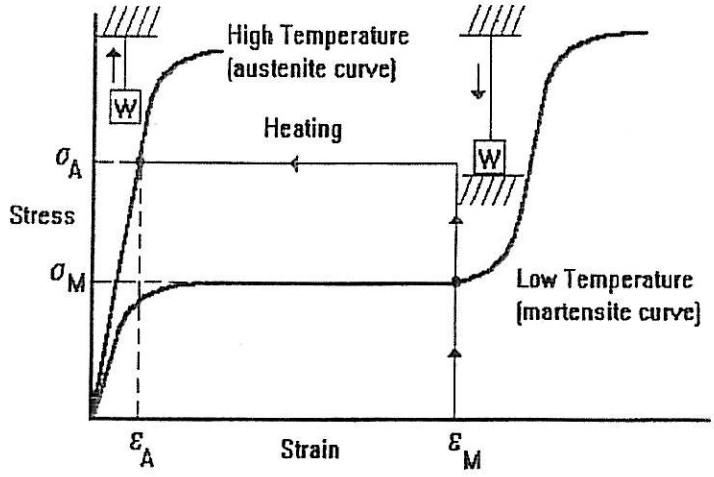

Figure 2.10 Stress-Strain Curves Illustrating the shape memory effect

Thus in Figure 2.10, the basic parameters upon which all shape memory alloy design are based. The point on the low temperature curve denoted by the coordinates σ_M and ε_M, represents the deformed state of a shape memory element.

2.4 Two-way shape memory

The ability of shape memory alloys to recover a preset shape upon heating above its transformation temperatures and return to an alternate shape upon cooling is known as two-way memory. Two-way memory is unique in that the material "remembers" different high temperature and low temperature shapes. Much has been written about this unique phenomenon in the literature and it has triggered many ideas in the minds of product designers. Some examples of these potential applications include reversible fasteners, temperature-sensitive actuators, retrievable medical implants, and toys and novelty items.

Creating two-way memory in Shape memory alloys involves a somewhat more complex training than with the one-way SMA.

2.5 Superelasticity

These unique alloys also show a Superelastic behavior if deformed at a temperature which is slightly above their transformation temperatures. This effect is caused by the stressinduced formation of some martensite above its normal temperature. Because it has been formed above its normal temperature, the martensite reverts immediately to undeformed austenite as soon as the stress is removed. This process provides a very springy, "rubberlike" elasticity in these alloys.

2.6 Setting shapes to SMA

The use of shape memory or superelastic element for a particular application generally requires the setting of a custom shape in a piece of SMA. The process required to set the shape is similar whether beginning with SMA in the form of wire, ribbon, strip, sheet, tubing, or bar. Shape setting (or training) is accomplished by constraining the SMA element on a mandrel or fixture of the desired shape and applying an appropriate heat treatment. The heat treatment methods used to set shapes in both shape memory and superelastic forms of SMA are similar.

2.7 Properties of Shape Memory Alloys

This section gives some properties of shape memory alloys. Table 2.1 gives the shape memory properties of nickel-titanium alloy as used in this research.

Table 2.1 Shape Memory Properties

Property	Austenite	Martensite
Melting temperature, ^{o} C (^{o} F)	1300 (2370)	
Density, g/cm^3 (lb_m/in^3)	6.45 (0.233)	
Resistivity, $\mu\Omega$ -cm	Approx. 100	Approx. 70
Thermal conductivity, W ^{o} C/cm (BtuHr ^{o} F/ft)	18 (10)	8.5 (4.9)
Corrosion resistance	Similar to 300 series stainless steel or titanium alloys	
Young's modulus, GPa (1000 ksi)	Approx. 83 (12)	Approx. 28 to 41 (4 to 6)
Yield strength , Mpa (ksi)	195 to 690 (28 to 100)	70 to 140 (10 to 20)

Ultimate tensile strength, MPa (ksi)	895 (130)
Transformation temperatures, ^{o} C (^{o} F)	-200 to 110 (-325 to 230)
Latent heat of transformation, KJ atom/kg (cal atom/g)	167 (40)
Shape memory strain	8.5% maximum

2.8 Alloy Systems

In this section gives some types of shape memory alloys, required for the actuators. Although there are at least 18 known alloy systems which exhibit the shape memory effect, at present only three are of commercial importance : Nickel-Titanium (Ni-Ti), Copper-Zinc-Aluminum (Cu-Zn-Al), and Copper-Aluminium-Nickel (Cu-Al-Ni).

2.8.1 Nickel Titanium

The nickel titanium alloys, generally reffered to as Nitinol, usually have compositons of approximately 50 atomic % Ni / 50 atomic % Ti, with small additions of copper, iron, cobalt, or chromium. One ternary alloy of notes is Ni/Ti/10 atomic % Cu. Nickel-titanium is about four times the cost of Cu-Zn-Al alloys, but it possesses several advantages over Cu-Zn-Al and Cu-Zn-Ni.

2.8.2 Copper-Zinc-Aluminum

The copper-zinc-aluminum have a composition of 15 – 25 weight % Zn / 6 – 9 weight % Al / balance Cu. Cu-Zn-Al has also been developed and lower in cost than nickel titanium, but they posses some inferior characteristics. Transformation temperatures can drift slightly during cycling and to significant extent if the alloy is not processed properly. These alloys are susceptible to stress corrosion crarking.

2.8.3 Copper-Aluminum-Nickel

Similar to Cu-Zn-Al, copper-aluminum-nickel has been developed as a quaternary alloy. The composition of Cu-Al-Ni is 13 – 14 weight % Al / 3 – 4 weight % Ni / balance Cu. Cu-Al-Ni alloys possess lower ductility than either Ni-Ti or Cu-Zn-Al. The

corrosion resistance is inferior to Ni-Ti and their cost is higher than Cu-Zn- Al. Cu-Al-Ni alloys also have the highest transformation temperatures of the three alloys.

2.9 All – Around Shape Memory Effect

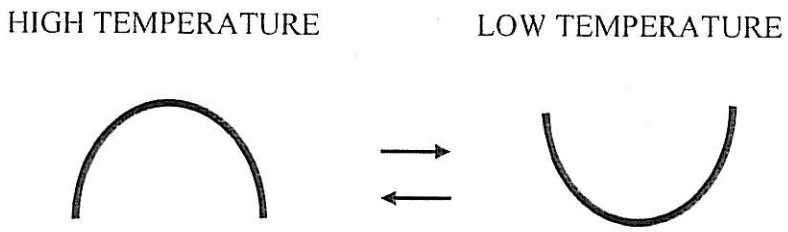

Figure 2.11 All-Around shape memory effect

Figure 2.11 shows the all-around shape memory effect. The all-around shape memory effect differs from the two-way effect in the following ways :-

(i) a greater amount of shape change is possible with the all-around effect. the high and low temperature shapes are exact inverses of each other, i.e., a complete reversal of curvature is possible in the case of piece of shape memory strip.

CHAPTER 3

CONVENTIONAL ACTUATOR

Three main types of actuation have been the core of motion and force power for all robotic systems. They are Hydraulic, Pneumatic, and Electric motors. These three come from two main types of power conversion. The first two are considered fluid machines in that they use fluid to create mechanical motion whereas the electric motor converts electrical energy into mechanical energy. The following will describe briefly, each actuation method with its advantages and disadvantages. Detailed description of these actuators can be found in many robotics and haptics textbooks such as [Stadler, 1995; Burdea, 1996]. A very good comparative study of actuators is robotics can be found in [Hollerbach, Hunter and Ballantyne, 1992].

3.1 Hydraulic Actuators

3.1.1 Principle of Operation

An actuator of this type works by changes of pressure. This system can be used in both linear and rotary actuation. The general linear mechanism consists of a piston encased in a chamber with a piston rod protruding from the chamber. The piston rod serves as the power transmission link between the piston inside the chamber and the external world. There are two major configurations of this actuator: single or double action. For the single action configuration, it can exert controllable forces in only one direction and uses a spring to return the piston to the neutral or un-energized position. Figure 3.1 shows a cut away view of a double action actuator which can be actively controlled in both directions within the chamber. In the case of rotary actuation, the power unit is a set of vanes attached to a drive shaft and encased in a chamber. Within the chamber the actuator is rotated by differential pressure across the vanes and the action is transmitted through the drive shaft to the external world.

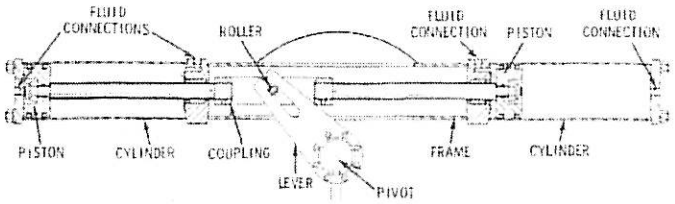

Figure 3.1 Drawing of Double Action Hydraulic Actuator

A representative closed loop position control for a linear hydraulic actuator is shown in Figure 3.2. The open loop dynamics of the hydraulic actuator are usually approximated with a first order system where the time constant depends on the piston

area A. The desired piston position X_d is compared to the actual position X. The obtained error E is processed by the controller which in most of the cases is a PID controller and the drive current I which will be the input to the servo-valve is obtained. Then the current I is multiplied with the flow gain K_q and the servo-valve no-load flow Q_0 is obtained. The Output Flow Q is the difference between Q_0 and a flow Q_d due to disturbance forces F_d which are mainly friction and gravity. Flow Q is the input to the hydraulic system that will result in a piston velocity V and a piston displacement X.

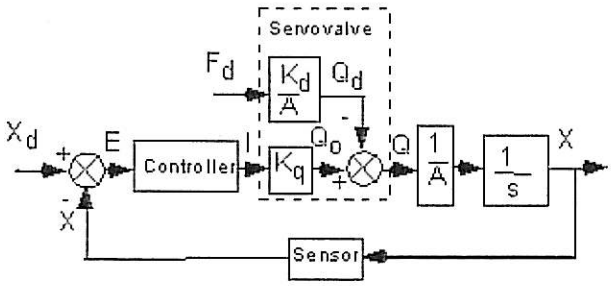

Figure 3.2 Closed Loop Position Control of a Hydraulic Actuator

It has to be noted that in Figure 3.2, the dynamics of the servo-valve have been approximated with very simple linear relationships. This representation can be realistic in low frequency operations. However, in high frequencies, electro-hydraulic servo-valves can exhibit highly non-linear dynamics. [Hollerbach, Hunter and Ballantyne, 1992].

Hydraulic manipulators are mainly used in applications where large robotic systems with high payload capability are needed. Examples are nuclear and underwater applications. A hydraulic manipulator that is currently used in many different heavy duty industrial and field tasks is shown in Figure 3.3 The TITAN 3 by ALSTOM Automation Schilling Robotics [Schilling, 1999] is extensively used for underwater applications on remotely operated vehicles (ROVs). The seven-function TITAN 3 has the dexterity and accuracy necessary to perform the fine movements needed for complex tasks. When this

ability is combined with the manipulator's reach (1,915 mm or 75.4 inches), payload capacity (113 kg at full extension), depth rating (available up to 6,500 msw), and large operating envelope, the TITAN 3 offers unequaled performance in a wide range of subsea applications. The TITAN 3 is constructed primarily of titanium for structural strength, light weight, and corrosion resistance.

3.1.2 Advantages – Disadvantages

One of the main advantages of hydraulic actuators is that these systems can deliver a great deal of power compared to their actuator inertia. Other aspects, which make a hydraulic actuator useful are the low compressibility of hydraulic fluids and, the high stiffness which leads to an associated high natural frequency and rapid response. This means that the robot using hydraulic actuators can execute very quick movements with great force. Additionally they tend to be reliable and mechanically simplistic as well as having a low noise level, and relatively safe during operation. As for this method of actuation, design characteristics are well known so the process of design is made easier due to this extent of knowledge.

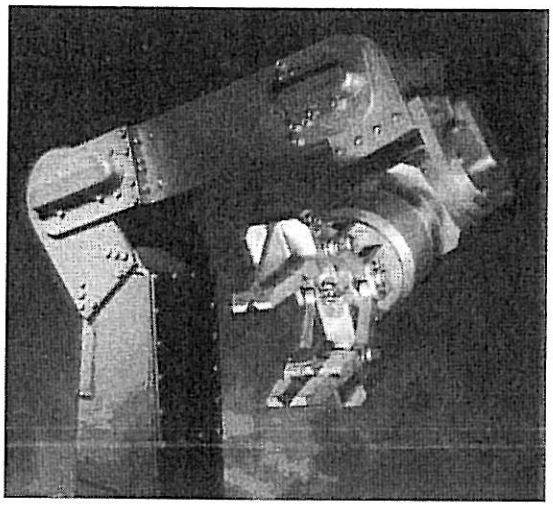

Figure 3.3 Schilling TITAN 3 Manipulator

One of the larger concerns with hydraulic systems is the containment of the fluid within the actuation system. Not only is this because of the contamination of the surrounding environment, but the leakage can also contaminate the oil and possibly lead to damage of interior surfaces. Additionally, the hydraulic fluid is flammable and pressurized so leaks could pose an extreme hazard to equipment and personnel. This adds the undesirable aspect of additional maintenance to maintain a clean sealed system. Other drawbacks include lags in the control of the system due to the transmission lines and oil viscosity changes from temperature. In fact, such temperature changes in the fluid can be drastic enough to form vapor bubbles when combined with the changes in fluid pressure in a phenomena called cavitation. During operation as temperature and pressure fluctuate, these bubbles alternately form and collapse. At times, when a vapor bubble is collapsing, the fluid will strike interior surfaces which had vapor filled pores and high surge pressures will be exhibited at the bottom of these pores. This bubble collapsing can dislodge metal particles in the pore area and leave a metallic suspension within the fluid. The degradation of the interior surfaces and the contamination of the fluid result in a marked drop in the performance of the system.

3.2 Pneumatic Actuators

3.2.1 Principle of Operation

These type of actuators are the direct descendents of the hydraulic systems. The difference between the two is that pneumatic systems use a compressible gas (i.e. air) as the medium for energy transmission. This makes the pneumatic system more passively compliant than the hydraulic system. With pneumatic actuators, the pressure within the chambers is lower than that of hydraulic systems resulting in lower force capabilities. In Figure 3.3 there is a cut away view of the basic pneumatic actuator. It is quite similar to the hydraulic counterpart however there are no return hydraulic lines for fluid. In a typical actuator of this type the fluid, namely air, is simply exhausted through the outlet valve in the actuator. Digital control of pneumatic systems is very similar to hydraulics with some exceptions to gains and stiffness constants (see also Figure 3.1)

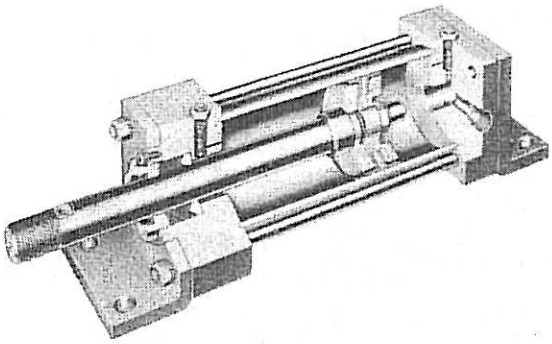

Figure 3.4 Cutaway View of Pneumatic Actuator

Pneumatic systems have been used in robotic systems when lightweight, small size systems are needed with relatively high payload to weight ratio. Examples of applications include walking machines and haptic systems. In Figure 3.5, a six-legged,

pneumatically powered walking robot is shown [Binnard, 1995]. The pneumatic actuation system provides lightweight, powerful actuators. The robot's mechanical structure is a lightweight frame built from carbon fiber and aluminum tubing and injection molded plastic. Preliminary results indicate that Boadicea walks faster, and can carry more payload, than previous small walkers. Boadicea has six legs powered by compressed air at 100 psi.

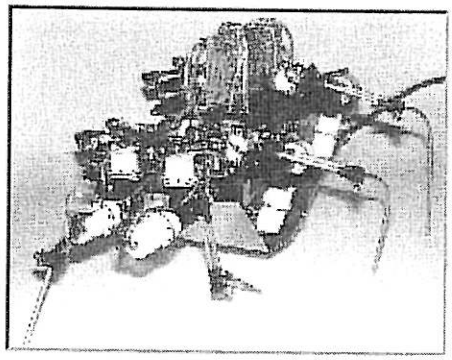

Figure 3.5 Boadicea: a Six-Legged Pneumatic System

3.2.2 Advantages – Disadvantages

Pneumatic actuators have less force capability than hydraulic actuators. Since, in contrast, the system operates at a lower pressure than the hydraulics and does not require return lines for the fluid, the support structure of the manipulator is much lighter than the other system. Pneumatics are cleaner and nonflammable which makes its uses in certain environments (i.e. – cleanrooms, operating rooms) more desired. Additionally, installation, operation and maintenance is easier and cost is lower.

Though the lack of hydraulic fluid makes this system cleaner, it has the disadvantage of not having a self-lubricating actuator. This generally means that pneumatic systems have a high friction force to overcome in order to maneuver and the diversion of power to combat friction gives these systems a lower working force. The release valve that allows pressurized air to escape has a tendency to be load if a muffler is not employed. Of course due to the medium which is compressible, control of motion is handled differently than hydraulics. While compliance is desired in a hydraulic system, force and speed are wanting in a pneumatic setup therefore the methodology to get these performance aspects is left to ingenuity of software control and nozzle design.

3.3 Electric Actuators

3.3.1 Principle of Operation

Of the three types of conventional actuator systems, electric motors have the largest variety of possible devices such as: Direct Current (DC) motors and their variants (brushed and brushless, low inertia, geared and direct drive, permanent magnet), Alternate Current (AC) motors, Induction Motors, and Stepping Motors. By definition, the principle behind an electric motor is a simple one, which is the application of magnetic fields to a ferrous core and thereby inducing motion.

A schematic of an AC motor and of a two-pole induction motor is shown in Figure 3.7 and of a DC motor in Figure 3.8. An AC motor is comprised of an electromagnet positioned above a permanent magnet which is mounted on a pivot. When current is sent through the coil, the permanent magnet rotates so that opposite poles align.

As the AC current switches direction, the permanent magnet continues rotation to align with reversed poles.

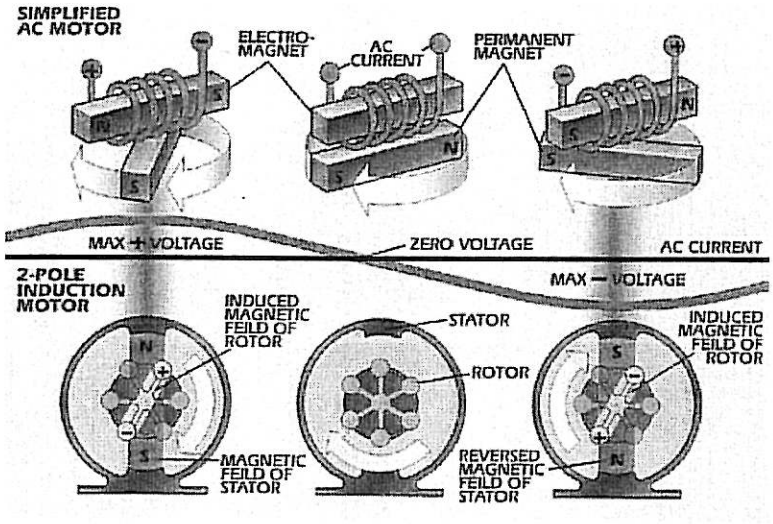

Figure 3.6 Basic Operation of a DC induction motor

A two-pole induction motor, shown in Figure 3.6, has a rotor which is the inner part that rotates and a stator of a permanent magnet composed of two or more permanent magnet pole pieces. The rotor is composed of windings which are connected to a mechanical commutator. The opposite polarities of the energized winding and the stator magnet attract and the rotor will rotate until it is aligned with the stator. Just as the rotor reaches alignment, the brushes move across the commutator contacts and energize the next winding. Notice that the commutator is staggered from the rotor poles. If the connections of a motor are reversed, the motor will change directions. DC motors are very similar to induction motors. The only difference is that a current is sent to the armature through contact between brushes and commutator. Spinning commutator acts as a reversing switch that alternates magnetic field.

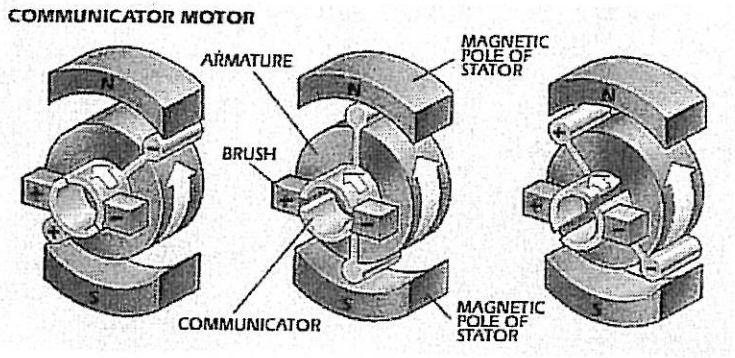

Figure 3.7 Block diagram of a DC motor

A position control scheme, in the Laplace domaine, for a permanent magnet DC motor is shown in Figure 3.7. The desired motor position Θ_d (and velocity) is compared to the actual position Θ (and velocity) that is usually obtained using angular position sensor such as optical encoders or potensiometers. This comparison yield the position (and velocity) error E that is processed by the controller. Usually, a PID controller is used and is designed to achieve fast and accurate response with no overshoot. The output of the controller is the voltage V that will be the input to the DC motor. Voltage V will be reduced by the "back emf" voltage V_b which is created by the angular motion of the motor shaft. The back emf voltage is proportional to the angular velocity Ω and the coefficient of this linear relationship is called the "back emf constant" K_b. The open loop dynamics of the motor are distinguished into the dynamics of the electrical part and of the mechanical part. The electrical circuit dynamics are approximated using a first order system where L is the armature inductance and R is the armature resistance. The armature current I which is the output of the electrical part. will result in the motor torque τ_m. The relationship between I and τ_m is linear and the coefficient K_i of this linear relationship is called the "motor constant". The sum of the motor torque τ_m with the disturbance torques τ_l felt by the motor shaft will be the input to the mechanical part of a DC motor. The disturbance torques τ_l are due to the load carried by the motor, friction and elastic effects at the payload level and other dynamic effects that have not been taken into account by the model. The coefficient n is the gear ratio and divides any torques due to

the payload. The dynamics of the mechanical part are of second order, including a motor inertia J_m and a friction term with friction coefficient B_m. A detailed description of the control of a DC motor can be found in [Spong and Vidyasagar, 1989].

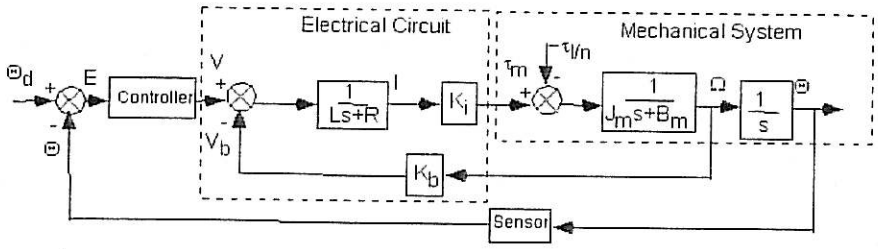

Figure 3.8 Position Control of a DC Motor

3.3.2 Advantages – Disadvantages

Since the energy medium for electric motors is easily stored and re-supplied by recharging batteries if mobility is needed, this makes electric motors the best choice when it comes to portability. Concurrently, as far as energy mediums, electric motors' power source is more adaptable to environments than hydraulics or pneumatics since volumetrically they take up less space. There are no hydraulic return lines, air lines, high pressure pumps, or reservoir tanks as in the case of the previously described systems. In tasking a robot to perform difficult maneuvers, the flexibility of control of the mechanical system with electric motors is far greater. This is because of the energy medium can be used by both the control system and the manipulator directly. They are also easy to install, clean (no leaks) and relatively quiet when they are compared to the hydraulic and pneumatic actuators.

The major disadvantage of electrical motors is that they produce very small torques compared to their size and weight. As the trend in robotics is to build smaller robots that are very powerful, electrical motors seem to be not suitable for such applications. Table 3.1 gives a broad scope view of the three types of conventional actuators studied in this section. Figure 3.9 compares the power density versus the weight of several conventional actuators and of the Shape Memory Alloy actuators that are discussed in the next chapter

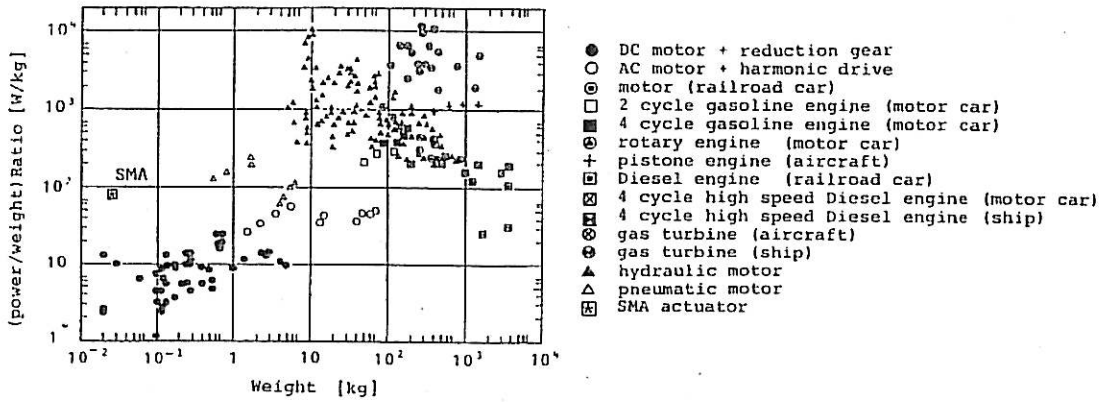

Figure 3.9 Power Density vs. Weight of Several Actuators

Table 3.1 Comparison of Conventional Actuators

Factor	Electrical	Hydraulic	Pneumatic
1. Basic system	Solid State Logic, Power Amplifiers, DC or AC Motors, Gear Boxes, Ball Nuts, Coolers	Pump, Sump, Regulators (Pressure, Temp., Flow), Filters, Heat Exchangers,	Compressor, Interstage Coolers, Pressure Controls, Filter, Dryers, Mufflers, Valves, Actuators,

		Servo Valves, Motors, Actuators, Accumulators	Snubbers
2. Working principle	Electricity	High quality oil base with additives, Water based solutions, Synthetic liquids	Air, Nitrogen, Combustion products
3. Efficiency	Over 90% for Large Systems	Seldom over 60%	Seldom over 30%
4. Susceptability to contamination	*Low:* (Electrical Line Noise +/- 10%) Easily handled RFI noise easily handled by shielding and filtration	*High:* Filters required special handling during maintenance. Cleaning procedures important. Servo valves easily damaged	*Intermediate:* Less trouble than oil. Particles drop out before getting to valves. Moisture & corrosion a problem.
5. Weight to force ratio	*Poor:* Motor & gearing must be carried by each sub-system. poorest weight to force ratio	*Excellent:* Highest force to weight ratio	*Fair:* Light weight, but low pressures produce intermediate force to weight ratio

6. Safety of Operation	Safest system electrical shock hazard & grounding must be considered	Leakage of flammable fluids & fire hazards high velocity jets of fluid can pierce skin, blood poisoning eye inflammations possible	Flying debris from ruptures can be very dangerous. Explosions possible when volatile oils are present (Nitrogen Non-Explos.)
7. Temperature Sensitivity and Heat Removal	Low temperature sensitivity in the operating range, but poor heat dissipation relative to Hydraulic	High temperature sensitivity due to viscosity changes. Differential thermal expansion can cause transient malfunctions. Excellent heat removal at remote heat exchangers	Low temperature sensitivity. Differential thermal expansion can cause transient difficulties. Heat removal is not normally a problem since systems vent to atmosphere
8. Input Power Supply	24 Volts to 460 Volts	50-5000 psi	5-500 psi
9. Load Variation Susceptability	Dry friction on output motors can cause small to intermediate steady state errors at null	Dry friction on outputs can cause small steady state errors around null	Serious steady state errors can occur around null position due to dry friction on output shaft

10. System Stiffness	Reasonably stiff- stiffness dependent on speed reduction concepts	The Stiffest, most responsive system for heavy loads	Very soft system (Hydraulic is 400 x Stiffer)

CHAPTER 4

SHAPE MEMORY ALLOY ACTUATORS

This chapter concerns about the shape memory alloys actuators. This chapter also discuss about the shape memory alloys actuators in robotic and commercial applications. Advantages and drawbacks in use of SMA actuation mechanism also are elaborated.

4.1 Introduction

The remarkable properties of Shape Memory Alloys lead to contemplate several industrial applications for shape memory electrically activated devices (actuators). The response time of SMA actuators is one of the critical characteristics which must be carefully analyzed and optimized in order to create competitive applications. Nevertheless, very little work related to temporal characteristics of SMA actuators has been published. Some of them are only of experimental nature. The others present

mathematic models of SMA actuators considering a constant temperature of phase transformation.

The methodology used to derive analytic models is presented. The analytic models are based on a simple energy balance with varying temperature during phase transformation. A finite element model with phase transformation is also developed for a non-stationary thermoconductivity analysis. Then, data calculated by finite elements and by the analytic models are compared with the results of an experimental study performed on a NiTi SMA wire activated by an electric current. The analytic models are employed to study the combined effect of electric current, phase transformation and heat exchange with the environment on the response time of SMA actuators.

4.2 Nickel Titanium Actuators

Nickel titanium can be self heated by passing an electric current through it. This is because the high resistive of 80 to 89 micro ohm-cm of nickel titanium. The response time is then highly dependent upon the amount of current used, the diameter, the ambient temperature, and the actuator configuration. Voltage requirement depend on the total resistance of the element, and as such depend on the diameter / length ratio, and the total length of the element. It is possible to apply direct D.C or A.C currents to a nickel titanium actuator, but care must be taken so that the maximum temperature reached is at or below 250 ^{o}C, in order to avoid thermal instability. The most successful application of Nickel titanium actuator component usually have all or most of the following characteristics:

(i) A mechanically simple design.

(ii) The shape memory component is in direct contact with a heating/cooling medium.

(iii) Friction is minimized and no complex stresses or stress concentrations are present.

(iv) A minimum force and motion requirement for the shape memory component.

4.3 Actuators Application

Shape memory actuator are considered to be low power actuators and such compete with bimetal, solenoid and max motors. The characteristic of different types of low power actuators are shown in Table 4.1 .

Table 4.1 The characteristic of low power actuators

Type	Temperature	Motion	Characteristic
Solenoid	-50 to +120 °C	Linear	- simple design - low cost
Bimetal	-40 to +600 °C	Bending	- low cost - linear response
Wax Motor	-40 to +180 °C	Linear	- high force - low cost

Shape Memory	-100 to +170 °C	Linear Torsion Bending	- linear response - high force/size - simple design - linear or non-linear - silent operation - electrical and thermal conrol

In general, shape memory wire actuators can provide relatively large forces but the stroke is very limited, unless it is practical to use relatively long section of wire. The use of shape memory can sometimes simplify a mechanism or device, reducing the overall number of parts, increasing reliability and therefore reducing associated quality costs. Shape memory such as nickel titanium can be electrically actuated relatively easily and have potential to replace solenoid in some application. Shape memory also relatively low output force per unit costs compared to solenoid, but they are both noisy and generate high inertial forces. In another situation, shape memory actuators generate less electromagnetic interference than solenoid. Application potential for shape memory actuator also exist in robotic. It is possible to use the variation in resistivity of the shape memory material for positional feedback.

4.3.1 Shape Memory Alloy Actuators in Robotic Applications

Using Shape Memory Alloy actuators provides an interesting alternative to conventional actuation methods. Their advantages create a means to drastically reduce the size, weight, and complexity of robotic systems. First of all, SMA actuators possess

an extremely high force to weight ratio. A Ni-Ti actuator can apply an actuation stress of 500 MPa (72.5 ksi). So, a 150 μ m diameter Ni-Ti wire can apply a force of 8.8 N which is 0.897 kg_f (1.99 lb_f). If the wire is 10 cm (3.94 in.) long it would weigh 11.4 mg (0.025 lb_m) and could contract 0.85 cm. So, the actuator can lift an object 78,000 times its own weight nearly 1 cm! Granted a simple electrical circuit is needed to heat the wire, but the force to weight ratio is still remarkable. Shape Memory Alloy actuators also are incredibly compact and simple. In the example described above, the actuator itself has a volume of only 0.002 cm^2. A SMA actuation system consists only of the SMA element and a heating and cooling method. The cooling method can be as simple as a combination of natural convection, conduction, and radiation. A final advantage is noiseless operation. Whereas conventional actuators produce a significant amount of noise, the SMA actuator is completely silent.

Shape Memory Alloy actuators do have disadvantages which must be thoroughly considered and analyzed prior to deciding to use SMA for an application. First of all, they operate with a low efficiency. A SMA actuator is effectively a heat engine where the material converts thermal energy directly into work. Therefore, the efficiency of the actuator cannot be greater than that of the Carnot cycle. The efficiency of the Carnot cycle is low in the temperatures where typical SMA actuator operate -- not exceeding 10% [Hirose, Ikuta, and Umetani, 1984]. Second, SMA actuators operate at a low bandwidth, meaning they are relative slow to cycle. The cycling time is primarily dependent on the heat transfer characteristics of the SMA "cooling system". The primary parameters that affect bandwidth are the temperature and type of surrounding medium, the convection of the surrounding medium, and the surface to volume ratio of the SMA elements. Depending on the environment, heat dissipation can be a problem.

For a high temperature, low convection environment, the heat transfer to the surrounding medium is reduced resulting in a lower bandwidth. For a low temperature or high convection environment, the heat transfer is improved and bandwidth is increased.

However, greater heat transfer also means that more power is needed to achieve actuation temperature. Another disadvantage of SMA actuators is the small absolute strains achieved by the SMA material. With only 8.5% strain available (for Ni=Ti), mechanisms actuated by SMA that are required to create large motions must be cleverly designed. Converting small motions into large motions comes with the unavoidable reduction in mechanical advantage. A final disadvantage, and topic of much research, is the difficulty controlling SMA actuators. The Shape Memory Effect is a highly non-linear phenomenon. Non-linearities enter the process through the hysteresis behavior described earlier, non-linear heat transfer, and any non-linear change in the parameters that affects the phase composition of the material (temperature, stress). Another control issue is that the entire deflection of a SMA element occurs over a small temperature range making accurate control in partial contraction difficult. Control is also difficult due to the structural elasticity of SMA actuators.

When designing a Shape Memory Alloy actuator for a mechanism, one of the first decisions is specifying the source of heat to actuate the SMA element. In certain specialized applications, the temperature of the surrounding medium can be used as a source of heat. This method provides a excellent option when designing mechanisms that regulate temperature. For example, a SMA element can be placed in a medium (say air) whose temperature needs to be controlled. The SMA element can be manufactured such that its actuation temperature corresponds to some critical temperature of the medium. When the medium reaches the critical temperature, the SMA element would actuate and possibly open a valve supplying more cooling. Here, the SMA element acts as both the sensor and the actuator. No electronics are needed in this incredibly simple system.

For other applications, the typical source of heat to achieve actuation temperature is joule heating by electric current. The electrical source can be either DC or AC. If AC, it should be at a frequency significantly higher than the bandwidth of the SMA actuated system to avoid displacement fluctuations. The current I that flows through a SMA

element with resistance R, due to a certain voltage drop V and the corresponding power P can be found from the following well-known relationships:

$$I = \frac{V}{R}$$

$$P = IV \text{ or } P = I^2R$$

Integrating a plot of power versus time and then dividing by the total time provides the average power. The average power required to achieve actuation temperature can be supplied by a steady or time varying signal. An example of a time varying signal that has been used extensively in electrical actuation is Pulse Width Modulation (PWM). The advantage of this method is more uniform heating of the SMA element. As expected, larger voltages/currents cause more rapid actuation.

Shape Memory Alloy material can be formed into almost any shaped actuator imaginable. All that is needed is a heat treatment process to define the actuators dimensional configuration in the austenite (actuated) phase. Some shapes that have been used are cantilever beams, wires, springs, ribbon, strip, sheet, and tubing. Although a SMA actuator could be designed such that it applies a force in three dimensions (depending on which direction it was deformed from the memory configuration), the great majority of SMA actuators apply a one directional tensile force and cannot directly apply a compressive force. In order to apply a compressive force, the actuator dimensions would have to be large enough to ensure rigidity and prevent buckling. As discussed earlier, large dimensions would cause a major decrease in the surface to volume ratio and, consequently, bandwidth. The end result is in order to have a SMA actuator with sufficient bandwidth, the SMA element must be thin, making it only capable of applying

tensile forces. Since most mechanisms require cyclic motions, a bias force is needed to return the mechanism in the opposite direction from which it was pulled by the SMA actuator. This bias force can be supplied by stored potential energy (gravity or a spring) or be provided by another SMA actuator working antagonistically. Simple examples of bias force are shown in Figure 4.1. Some excellent basic design principals for single element SMA Actuators can be found in [Waram, 1993].

The very simple mechanisms in Figure 4.1 can achieve only small linear motions. In order to achieve large motions, a SMA actuator must be cleverly attached to the mechanism it operates. For a simple mechanism consisting of a moving link that pivots about a fixed revolute joint, the small linear displacements of a SMA actuator can be converted into large angular motions by fixing one end of the actuator and attaching the free end to the moving link close to the center of rotation of the revolute joint. This is very similar to the way biological muscles move the links that make up the body. Of course, mechanical advantage is lost as the free end of the actuator approaches the center of rotation.

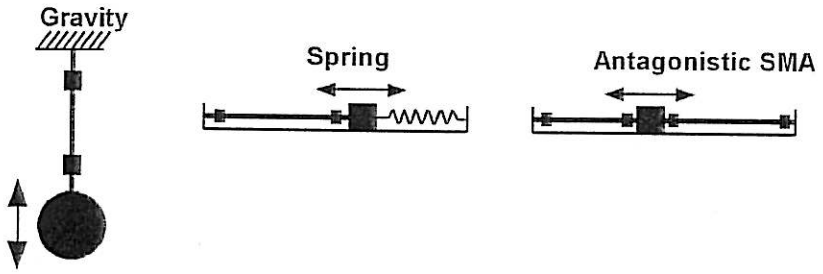

Figure 4.1 Examples of Bias Forces in SMA Actuated Systems

Application of these SMA actuators is already used in robotics technology, most originating in Japan, over the last 5-10 years. One example of the robot was developed used shape memory actuator is a "crab" robot for undersea mining of manganese nodules has also been proposed as an application for nickel titanium actuators.

4.3.2 Shape Memory Alloy Actuators in Others Applications

Besides robotic applications, fire protection is another area of shape memory alloys actuators application. Shape memory wires have been used as electrical sensors for fire protection. The advantages of shape memory actuators for fire protection is that they respond to an increase in ambient temperature and so can provide some degree of advance warning of a fire.

An SMA-actuated gripper also was developed for use in semi-conductor wafer transportation in a clean-room. The lack of moving parts and simple construction help to maintain the dustless environment required for wafer production. Indeed, the number of application and obvious advantages seem to indicate that SMA will be a permanent addition to the repertoire of robotics actuators. One other possible area of shape memory actuator application is circuit breaker. Resettable short circuit protection is difficult for shape memory actuators since a high temperature is usually involved and this tends to damage the shape memory element or at least seriously degrades its action. Because the response is thermal, the use of shape memory actuators can eliminate false tripping due to electrical surges, since the surges is "smoothed out" by heat transfer.

Another typical actuators application configuration are plentiful of miniaturization made possible through the use of shape memory alloy spring:

(i) Shape memory controlled valve
(ii) Shape memory air vent controller
(iii) Shape memory latching mechanism
(iv) Shape memory bell crank mechanism
(v) Shape memory microswitch controller

4.4 Typical Shape Memory Actuator Configuration

Figure 4.2 shows a typical valve application in which the fluid flow is perpendicular to the action of the shape memory spring

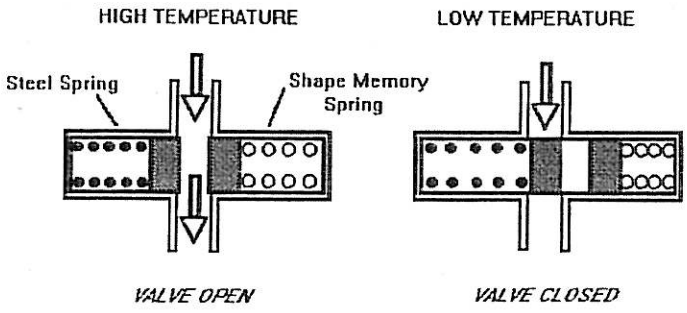

Figure 4.2 shape memory controlled valve, perpendicular action mode

Figure 4.3 illustrates the operation of a latching valve, which could be used as a safety mechanism to cut off gas flow in the event of a fire or an extreme temperature increase. Shape memory spring is used to release the valve mechanism, so it only has to work against friction.

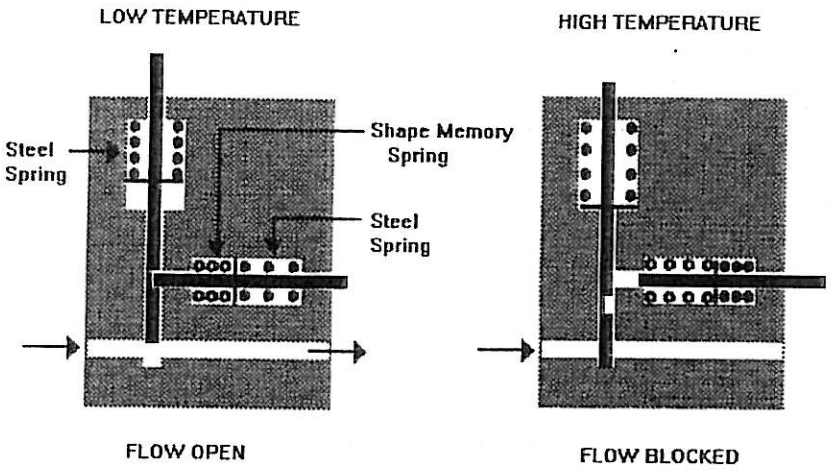

Figure 4.3 shape memory Latching mechanism

Shape memory spring can be used to control a bell crank is shown in the Figure 4.4. By changing the dimension of the bell crank, to adjust the mechanical advantage, various combinations of force and motion can be obtained.

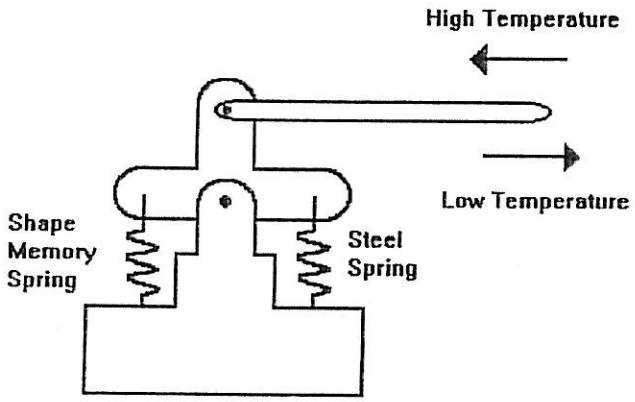

Figure 4.4 shape memory bell crank mechanism

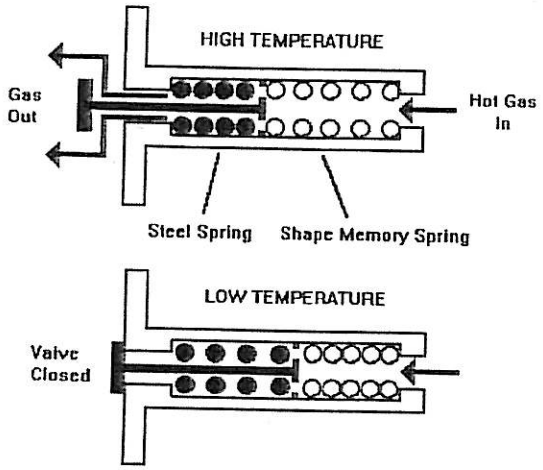

Figure 4.5 Shape memory controlled Valve, Parallel action Mode

A valve application in which the fluid flow is parallel to action of the shape memory spring shown in Figure 4.5 above.

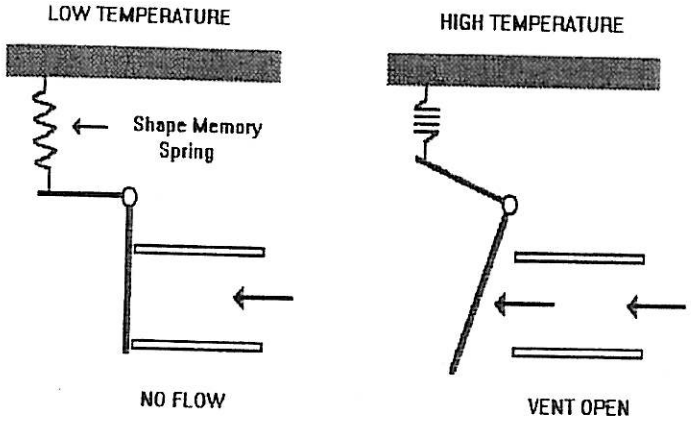

Figure 4.6 Shape memory air vent controller

Figure 4.6 shows a shape memory spring used to open and close a forced air vent. As a final example of a typical application shape memory actuator configuration, shape memory strip used to provide thermal control of a microswitch (Figure 4.7).

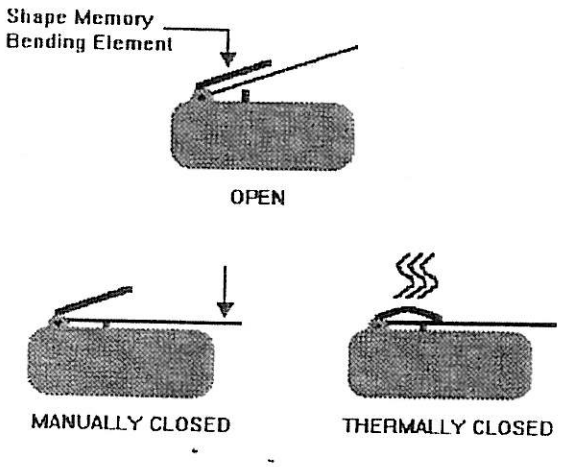

Figure 4.7 shape memory Microswitch controller

4.5 Advantages in use of SMA actuation mechanisms

SMA offer important advantages in actuation mechanisms, as summarized below.

4.5.1 Simplicity, compactness, and safety of the mechanism

The actuator can be reduced to a single SMA element, i.e. an electrically activated SMA wire. The stroke and force can be easily modified by the selection of the SMA element, e.g. SMA wire vs. SMA spring. Additional parts such as reduction gears are not required. Hence, the use of SMA can result in a simplified, more compact and more reliable device.

4.5.2 Creation of clean, silent, spark-free and zero gravity working conditions

Since friction is absent in activated SMA elements, the production of dust particles can be avoided. Conversely, a dusty environment has no influence on the action of SMA elements. Since there are also no additional vibrating parts, the activation is nearly noiseless. While no high-voltage or electrical switches are required, SMA actuators can work completely spark-free allowing them to operate in highly inflammable environments. SMA actuators 5 can be controlled in such a way that accelerations of the order of only a few μ g are generated. These very smooth movements are therefore extremely suitable for space applications where even small accelerations can influence the global movement of satellites.

4.5.3 High power/weight (or power/volume) ratio's

This means that shape memory alloys are extremely attractive in microactuator technology. Therefore, it is expected that SMA-actuators will become a very important design tool in the important and rapidly growing field of micro-actuation.

4.6 Drawbacks in use of SMA actuation mechanisms

Some drawbacks on the use of SMA-actuators should however also be considered:

4.6.1 Low energy efficiency

It can be easily calculated that the maximum theoretical efficiency of a Carnot cycle between the temperature at which a shape memory alloy finishes transforming to Austenite upon heating and the temperature at which a shape memory alloy finishes transforming to martensite upon cooling is of the order of 10 %. In reality, the conversion of heat into mechanical work is much less efficient with the result that the real efficiency is at least one order smaller than the theoretical Carnot value

4.6.2 Limited bandwidth due to heating and cooling restrictions

Shape memory actuators can be heated in different ways, radiation or conduction (thermal actuators) and by inductive or resistive heating (electrical actuators). For a fast and homogeneous response, resistive heating offers the most attractive solution and is therefore also widely used. The response speed is mainly limited by the cooling capacities

4.6.3 Degradation and fatigue

The reliability of shape memory devices depends on its global lifetime performance. Time, temperature, stress, strain, strain mode and the amount of cycles are in this respect important external parameters. Internal parameters that can have a strong influence on the lifetime are: the alloy system, the alloy composition, the heat treatment, and the processing. For general purposes, the maximum memory effect, strain and/or stress, will be selected depending on the required amount of cycles. The following table, presented by D. Stöckel in 1992 can be used as a guideline for standard binary Ni-Ti alloys. It should however be remarked that special treatments and ternary alloys such as Ni-Ti-Cu can yield much higher values of maximum strains and stresses.

4.6.4 Complex control

Shape memory alloys show a complex three dimensional thermomechanical behavior with hysteresis. Moreover, this behavior is influenced by a large number of parameters. It follows that there are in general no direct and simple relations between the temperature and the position or force. Therefore, accurate position or force control by SMA actuators requires the use of powerful controllers and the experimental determination of complex data. Many mathematical models are being developed nowadays by different research groups to overcome this important limitation.

CHAPTER 5

DESIGN OF SHAPE MEMORY ALLOYS WIRE ACTUATORS

5.1 Introduction

Wire actuators can deliver considerably more force than spring actuators, but the amount of stroke is very limited. Again it is assumed that a linear stress-strain behavior exists for design purposes. The stress-strain-temperature behavior is depicted in Figure 5.1.

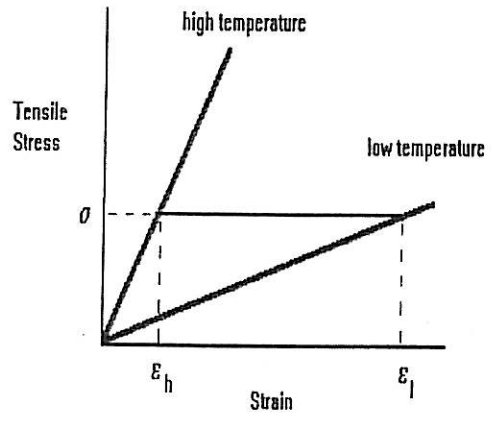

Figure 5.1 Stress-Strain Temperature Behavior

The slopes of the lines in Figure 5.1 represent the Young's modulus of the material. It can be seen that there is a dramatic increase in modulus with temperature, as noted previously. Referring to Figure 5.1, if the material is subjected to a stress of σ at low temperature, it loads along the low temperature line to a strain of ε_l. When the material is heated to the high temperature state, the strain will be recovered to ε_h, and the wire contracts as a result of the increase in modulus.

For design calculations, wire diameter and length are found by constraining the maximum tensile stress (at high temperature) and strain (at low temperature) to values which will ensure that the required fatigue life for the wire is obtained.

5.2 Design Method of Shape Memory Wire.

Unlike the simple model which assumes linear stress-strain behavior, a more detailed design method uses the actual stress-strain curves at high and low temperature for design calculations. Figure 5.2 illustrates typical stress-strain curves, and the design parameters.

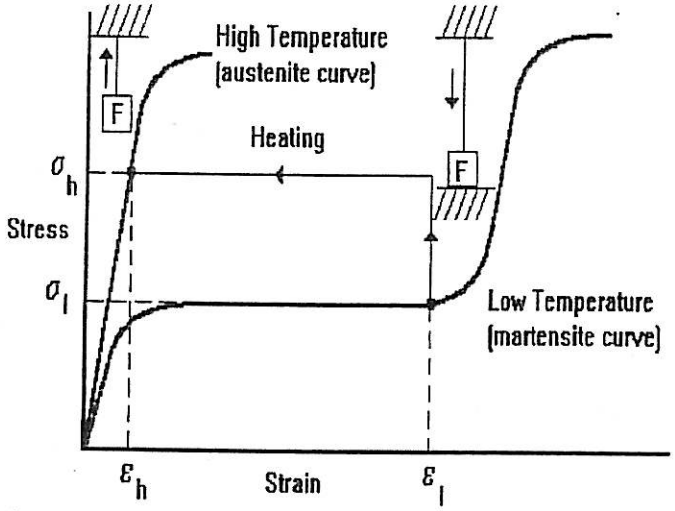

Figure 5.2 Straight Wire Design Curves

The design parameters are defined as follows:

σ_h = tensile stress in austenite condition

ε_h = strain in austenite condition

σ_l = tensile stress in martensite condition

ε_l = strain in martensite condition

The wire diameter, d, is determined by choosing the austenite tensile stress, σ_h, and by using the required actuation force, F:

$$\mathbf{d} = \sqrt{\frac{4F}{\pi\sigma_h}}$$

A typical value of σ_h, used for NiTi wire actuators is 170 MPa.

The strain in the wire when its in the austenite condition, ε_h, is found from the high temperature, stress-strain curve, by dropping a vertical line to the strain axis from the point where the austenite tensile stress value, σ_h, intersects the high temperature (austenite) curve.

The designer must next choose a low temperature strain, ε_l, appropriate for the expected cyclic life of the wire actuator. Typically, a value of 2% or $\varepsilon_l = 0.02$ is used if a high cyclic life is required. Recommendations concerning the appropriate values of ε_h and σ_h, for desired cyclic life expectancies, as well as the actual stress-strain curves, should be obtained from individual shape memory wire vendors.

The required wire length, L, is determined by:

$$L = \frac{stroke}{\varepsilon_l - \varepsilon_h}$$

The high temperature length of the wire, L_h, is given as:

$$L_h = (1 + \varepsilon_h) \times L$$

The low temperature length of the wire, L_l, is given as:

$$L_j = L_h + \text{stroke}$$

The low temperature stress, σ_l, {martensite condition} is found by drawing a horizontal line to the stress axis, from the point where the low temperature strain, ε_l, intersects the low temperature stress-strain curve.

The low temperature reset force is found as:

$$\text{Reset force} \doteq \frac{\sigma_l \pi \times d^2}{4}$$

Typical values for σ_l for NiTi alloys range from 70 MPa to 140 MPa, depending on alloy composition and heat treatment.

Assume that a straight wire Ni-Ti actuator must be designed which will raise a 100 N weight a distance of 2.5 mm, when a temperature change occurs from 20 to 100 °C. A cyclic life of 15000 cycles is required. A maximum design stress of 140 MPa will be used, to ensure good cyclic life.

The wire diameter, d, is determined as follows:

$$\mathbf{d} = \sqrt{\frac{4F}{\pi\sigma_h}} = \sqrt{\frac{(4)(100)}{(\pi)(140)}} = 0.95 \text{ mm}$$

The wire length, L, will be calculated assuming a low temperature strain, ε_l, of 2% or 0.02. The high temperature strain, ε_h, is determined as:

$$\varepsilon_h = \frac{\sigma}{E_h} = \frac{140}{59000} = 0.00237$$

where E_h is the value of the Young's modulus for the material at high temperature, in MPa.

The wire length is determined as:

$$L = \frac{stroke}{\varepsilon_l - \varepsilon_h} = \frac{2.5}{0.02 - 0.00237} = 141.8\text{mm}$$

The length increment needed at 100°C to produce the 100 N force is given by:

$$\text{Length increment} = \varepsilon_h \times L = 0.00237 \times 141.8 = 0.336\text{mm}$$

The low temperature stress, σ_l, is found as:

$$\sigma_l = \varepsilon_l \times E_l = 0.02 \times 6900 = 138 \text{ MPa}$$

where E_l is the value of the Young's modulus for the material at low temperature, in MPa. The reset force is found as:

$$\text{reset force} = \sigma_l \times \text{wire area} = 138 \times \frac{\pi \times d^2}{4}$$

$$= 138 \times \frac{\pi \times (0.95)^2}{4} = 97.8 \text{ N}$$

CHAPTER 6

EXPERIMENTAL & CONTROL SYSTEM

This chapter describes the experimental system has been developed for position control using a single SMA wire actuator, under constant load. The result of this system is presented for showed interesting non-linear dynamic characteristics of the actuator.

6.1 Physical System

In order to determine the performance characteristics of the wire SMA actuator was designed and constructed. An experimental has been developed using a single SMA wire actuator, under constant load. The experimental setup is shown in Figure 6.1.

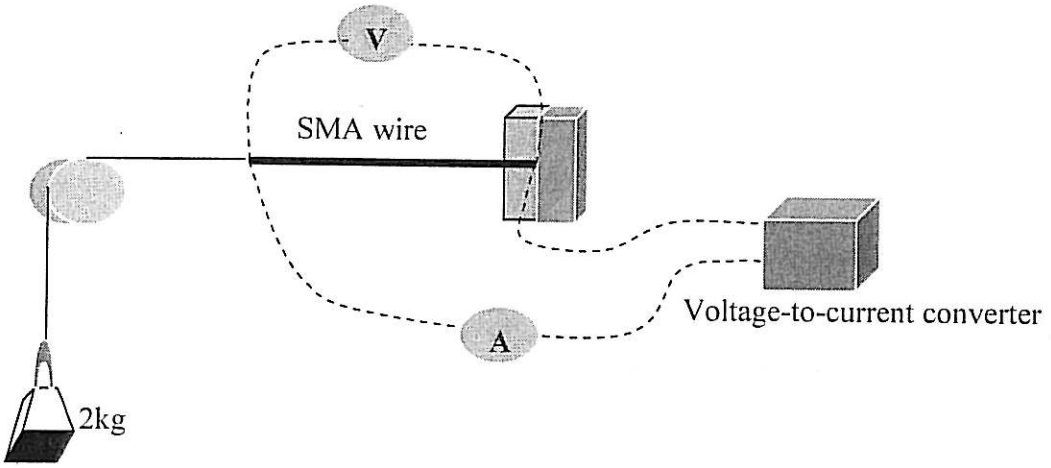

Figure 6.1 One-Wire Position Control System

The experiment consist of a 20 cm, 30cm length of 0.5 mm diameter NiTi wire, biased by a load of 2 kg. The load is chosen such that the SMA wire is stretch. This represent a constant stress on the wire of roughly 100 MPa. The wire is also assumed to be heated by an electric current. Dynamic measurements are made of the wire current, voltage and contraction, while control current is driven through the SMA by a voltage-to-current convert with grounded load. This system is assumed that the SMA wire is exposed to a constant ambient temperature and natural convection cools the wire. L_2-stability of position control system is also shown for the particular example of a semiactive proportional controller.

6.1.1 Voltage-to-current converter with grounded load

The voltage-to-current converter is shown in Figure 6.2. In this circuit, one terminal of the load is grounded, and load currents is controlled by an input voltage.

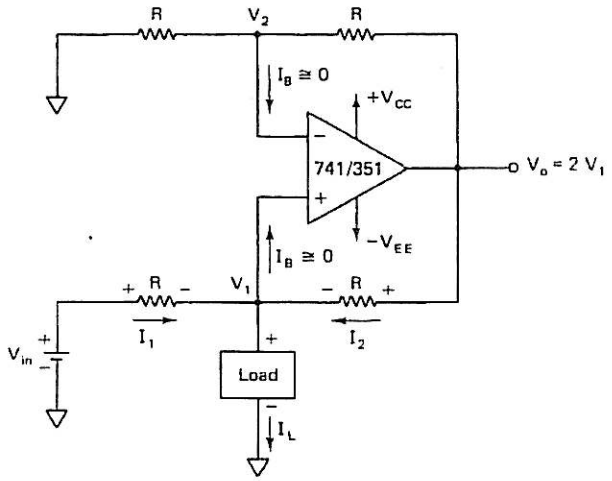

Figure 6.2 Voltage-to-current converter with grounded load

That is,

$$V_m = I_L R$$

Or

$$I_L = \frac{V_m}{R}$$

The load current depends on the input voltage V_m and resistor R.

6.2 Control system

The control system implemented on the setup of Figure 6.1 is represented in Figure 6.3. Here, the system blocks are labeled G_2 (controller) and G_3 (SMA wire), for later consistency.

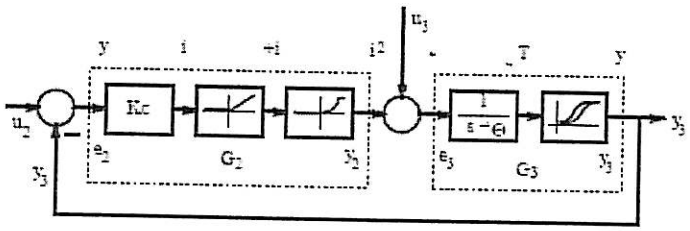

Figure 6.3 P^+ Control Loop

In the one-wire, constant-load configuration, only wire contraction can be actively controlled, through Joule heating by the wire current. The controller is modeled by a constant gain K_c (amp/cm), followed by an ideal diode block, which has unity slope for positive inputs and zero output for negative inputs. The current output is limited to i_{sat}, in order to prevent the wire from overheating. The conversion from current to power, as well as this saturation, is modeled by the quadratic block. The controller will be considered a relation $G_2 : L_{2c} \rightarrow L^{+}{}_{2c}{}^{1}$. To recognize its "positive" nature, the controller will be referred to as a P^+ controller. The model used for the wire behavior, G_3, convert "power" (i^2) to wire contraction. The power-temperature relationship is modeled as a

straightforward first-order transfer function, but the temperature-contraction behavior is non-linear, with hysterisis. Wire contraction is initialized to zero at room temperature, when the wire is stretched to the maximum strain. As it is heated, the contraction increases, but is bounded by the amount of recoverable strain. This gain dependent on the stress.

6.2.1 Stability

In this section, the stability theorem is applied to the system to determine stability condition for the position control system. A range of K_c will be stabilize the closed loop system for every dissipative G_1 for which $q < 0$. Before proceeding to the general problem, it is instructive to apply the dissipativity-based stability theorem to the P^+ control problem of figure 6.3.

6.2.1.1 P^+ control

Consider the system of figure 6.3. The dissipativity characteristic of two sub-blocks, are

G_2 is $(-d\beta,0,1)$ - dissipative $\forall d\beta \in (0,74(Ri_{sat}K_c)^{-1}$

G_3 is $(-\alpha_3,\alpha_3\gamma_3^{\,2},1)$ - dissipative $\forall \alpha_3 \geq 0$

The closed loop system of figure 6.3 is stable for all finite $K_c > 0$.

Proof

Consider an arbitrary, finite $K_c > 0$. Set

$$d\beta = \frac{74}{Ri_{sat} K_c} > 0$$

satistying the context bound on $d\beta$. To choose α_3 such that the two stability condition,

$$\alpha_3 > 0$$

and

$$\frac{74}{Ri_{sat} K_c} > \alpha_3 \gamma_3^{\,2}$$

hold. But, for all finite K_c, it is possible to choose

$$\frac{74}{Ri_{sat} K_c \gamma_3^{\,2}} > \alpha_3 > 0$$

For more general control law, consider the system of figure 6.4. G_1, a general mapping from L_{2e} to L_{2e}, has been inserted into position control loop of figure 6.3.

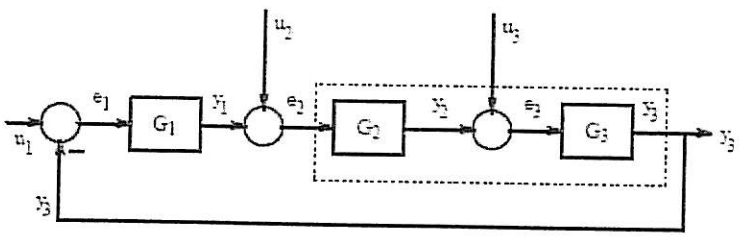

Figure 6.4 Generalized control loop

The G_1 assumed are dissipative with respect to some triplet (q, r, s). The dissipativity characteristic of sub-blocks are :

G_1 is (q, r, s) - dissipative

G_2 is $(-d\beta,0,1)$ - dissipative $\forall d\beta \in (0,74(Ri_{sat}K_c)^{-1}$

G_3 is $(-\alpha_3,\alpha_3\gamma_3^{\ 2},1)$ - dissipative $\forall \alpha_3 \geq 0$

The context bounds are identical to those of the P^+ control system, plus the assumption that G_1 is (q, r, s)-dissipative:

$$\alpha_3 \geq 0$$

$$d\beta > 0$$

$$d\beta \leq 0,74(Ri_{sat}K_c)^{-1}$$

The dissipativity of G_1 will be implicitly assumed.

6.2.2 Dissipativity characteristic of common controllers

This section demonstrates the calculation of the dissipativity characteristic of P, PI and PID controllers. These systems can be approximated by strictly stable, linear transfer functions. These characteristic will be implicit in the following discussion.

$$\|G\|_\infty \triangleq \sup_{\omega \geq 0} |G(j\omega)|$$

It is shown that the 2-norm to 2-norm gain of a linear system y = Gu is $\|G\|_\infty$.

That is,

$$\|y\|_2 \le \|G\|_\infty \|u\|_2 = \gamma \|u\|_2$$

As well, it is shown the pasivity coefficient can be calculated as

$$\delta = \inf_{\omega \ge 0} Rc\{G(j\omega)\}.$$

These results can be applied to the general form of the P, PI, PID controllers, to determine their dissipativity charaacterisic in term of their gain coefficients.

6.2.2.1 P Controller

The proportional controller has the form G = K_p. It is easy to see in this case, that $\|G\|$ = $K_p\|u\|$, and $\gamma = \delta = K_p$.

6.2.2.2 PI Controller

The form of the PI controller is

$$G(s) = K_p + \frac{K_i}{s + \varepsilon_i}$$

Calculating the gain gives

$$\begin{aligned} \gamma &= \sup_{\omega \geq 0} \lfloor G(j\omega) \rfloor \\ &= \sup_{\omega \geq 0} \left\lfloor K_p + \frac{K_i}{j\omega + \varepsilon_i} \right\rfloor \\ &= K_p + \frac{K_i}{\varepsilon_i}, \end{aligned}$$

and the dissipativity coefficient is

$$\begin{aligned} \delta &= \inf_{\omega \geq 0} Rc\{G(j\omega)\} \\ &= \inf_{\omega \geq 0} Rc\left\{K_p + \frac{K_i}{j\omega + \varepsilon_i}\right\} \\ &= \inf_{\omega \geq 0} Rc\left\{K_p + \frac{K_i(-j\omega + \varepsilon_i)}{\omega^2 + \varepsilon_i^2}\right\} \\ &= \inf_{\omega \geq 0} Rc\left\{K_p + \frac{K_i\varepsilon_i}{\omega^2 + \varepsilon_i^2}\right\} \\ &= K_p \end{aligned}$$

as $\omega \to \infty$. Assuming positive controller gain, both γ and δ are positive, and the controller is passive, with finite gain.

6.2.2.3 PD Controller

The form of the PD controller is

$$G(s) = K_p + \frac{K_d s}{\varepsilon_d s + 1}$$

Calculating the gain gives

$$\begin{aligned} \gamma &= \sup_{\omega \geq 0} \lfloor G(j\omega) \rfloor \\ &= \sup_{\omega \geq 0} \left\lfloor K_p + \frac{K_d j\omega}{\varepsilon_d j\omega + 1} \right\rfloor \\ &= K_p + \frac{K_d}{\varepsilon_d}, \end{aligned}$$

and the dissipativity coefficent is

$$\begin{aligned} \delta &= \inf_{\omega \geq 0} Rc\{G(j\omega)\} \\ &= \inf_{\omega \geq 0} Rc\left\{K_p + \frac{K_d j\omega}{\varepsilon_d j\omega + 1}\right\} \\ &= \inf_{\omega \geq 0} Rc\left\{K_p + \frac{K_d j\omega(-\varepsilon_d j\omega + 1)}{\varepsilon_d{}^2\omega^2 + 1}\right\} \\ &= \inf_{\omega \geq 0} Rc\left\{K_p + \frac{K_d \varepsilon_d \omega^2}{\varepsilon_d{}^2\omega^2 + 1}\right\} \\ &= K_p \end{aligned}$$

for $\omega = 0$. Again, assuming positive controller gain, both γ and δ are positive.

The P, PI and PD controllers have following dissipativity characteristic, for all $\alpha \geq 0$:

P is $(-\alpha, -K_p + \alpha K_p^{\,2}, 1)$ -dissipative

PI is $(-\alpha, -K_p + \alpha(K_p + \frac{K_i}{\varepsilon_i})^2, 1)$ - dissipative

PD is $(-\alpha, -K_p + \alpha(K_p + \frac{K_d}{\varepsilon_d})^2, 1)$ - dissipative.

In all three case, $\gamma \geq \delta$.

In the stability, three test controllers are considered, $G_1 = 1$, $G_1 = 10$, and $G_1 = 0.01 + \frac{0.0001}{s + 0.01}$. The first is of interesting in determining the conversativeness of the resulting gain since all strictly positive gains K_c should be stabilizing. For $G_1 = 10$ is instructive since, with K_c also a proportional gain, one might expect the total controller gain product G_1K_c to be the same as the K_c found for $G_1 = 1$. The stability result with PI controller was confined to the proportional controller. The simulaton results for this controller are shown in section 6.4.

6.3 Experimental results

In this section, the results of experimental are elaborated. Three different parameters were experimentally measured during the experiments:

(i) SMA wire voltage drop.

(ii) SMA wire current.

(iii) SMA wire contraction

Experimental results were shown in Figure 6.5 for voltages drop and fig 6.6 and 6.7, current response for SMA wire.

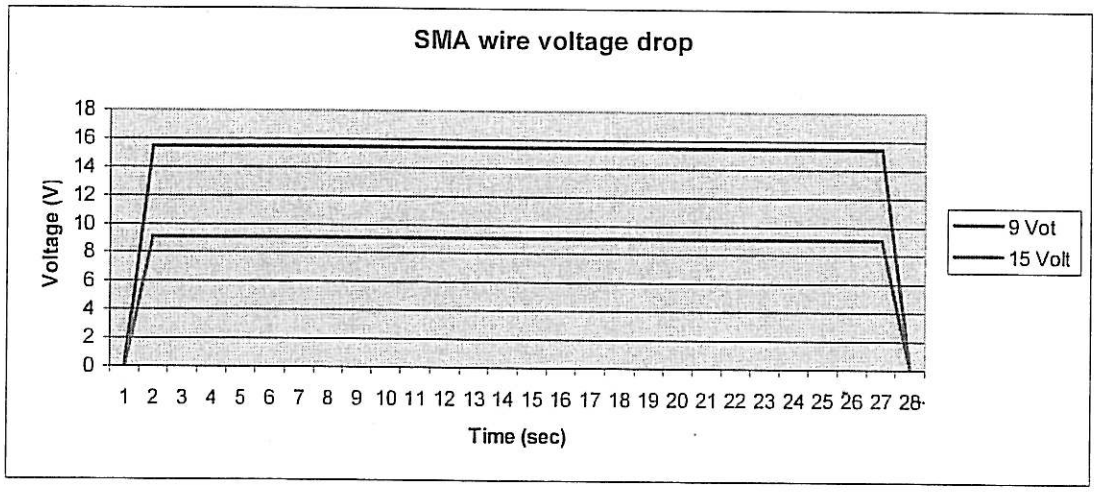

Figure 6.5 SMA wire voltages drop

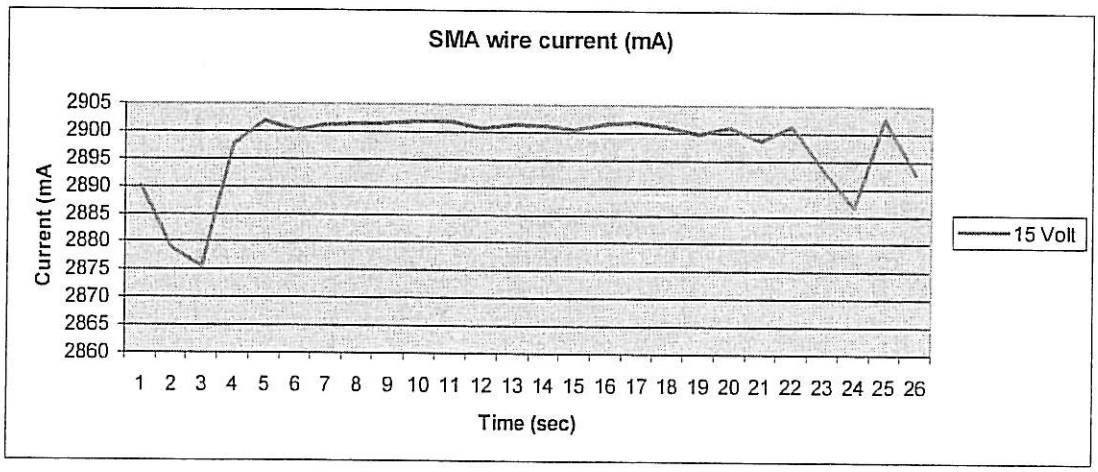

Figure 6.6 SMA wire current at 15 volt

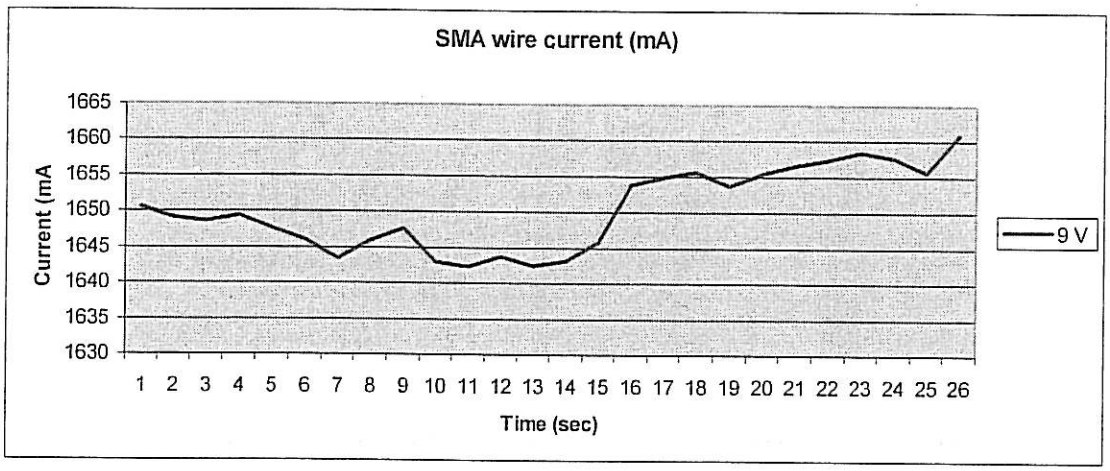

Figure 6.7 SMA wire current at 9 Volt

Figure 6.8 is shown a comparison of SMA wire current from the results in figure 6.6 and figure 6.7.

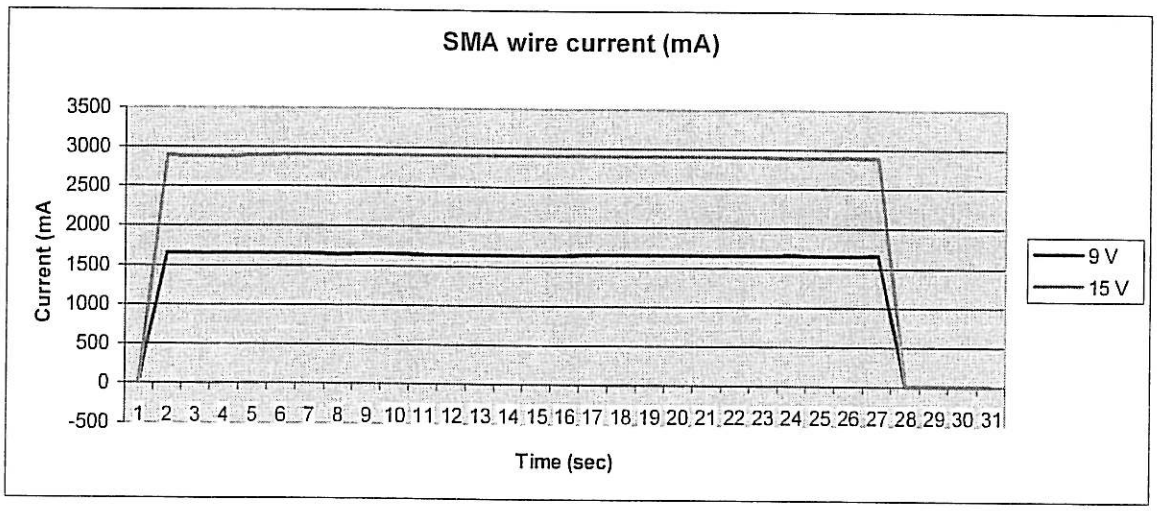

Figure 6.8 A comparison of SMA wire currents

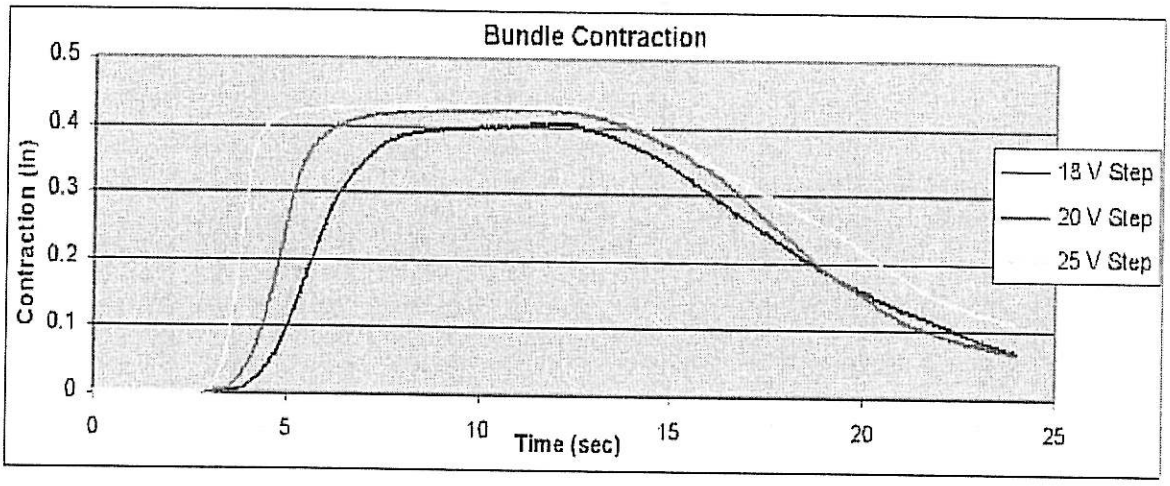

Figure 6.9 SMA wire contraction

Figure 6.9 shows the SMA wire contraction. The contraction wire has been observed occur so rapidly when the current supplied to SMA wire. This value will be constant until the cut-off of current supply, then the contraction will be decrease and back to the initial condition at a moment times.

6.4 Simulation results

Figure 6.10 and 6.11 shows are results of the two simulations using by proportional controllers, and are pretty much as expected. The gains calculated for the controllers $G_1 = 1$ and $G_1 = 10$ are 16.44 and 0.27, respectively. The steady state errors are close to those predicted by $\frac{100\%}{1+K}$, the formula for a step input. For $G_1 = 1$ the error is

4.66%, while $\frac{100\%}{1+G_1K_c}$ = 5.7 %. For G_1 = 10, $\frac{100\%}{1+G_1K_c}$ predicts 27% error, and the measured value is 27.45%.

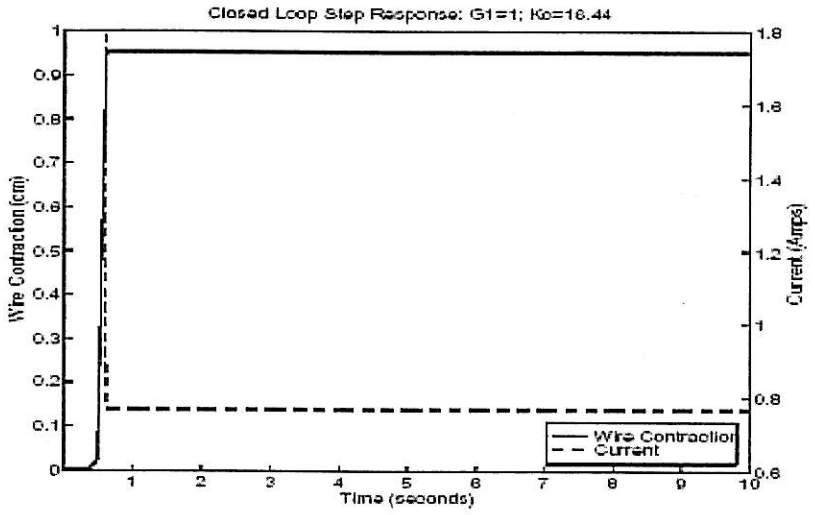

Figure 6.10 Closed Loop Step Response With G_1 = 1

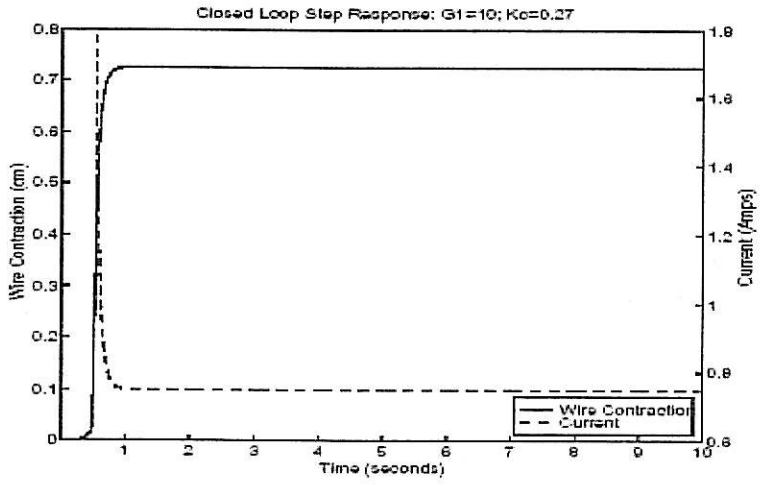

Figure 6.11 Closed Loop Step Response With G_1 = 10

6.3.1 PI Controller

For a controller using by PI controller the gain of controller was assumed as :

$$G_1 = 0.01 + \frac{0.0001}{s + 0.01}$$

If that controller were implemented on the experimental system, the maximum stabilizing gain calculated for that G_1 is 2.42. The results of simulation with $K_c^* = 2.42$ are shown in figure 6.12. The gain is obviously much too low active to achieve acceptable performance.

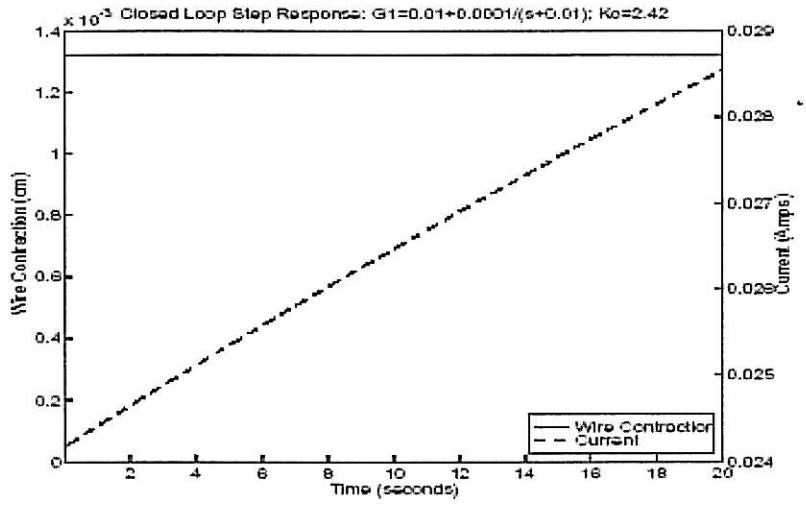

Figure 6.12 Closed Loop Step Response With $G_1 = 0.01 + \frac{0.0001}{s + 0.01}$

In comparing the results of proportional control simulations, it was seen that the optimization result is dependent on the gain distribution in the problem. To attempt to improve the gain K_c in G_2, the loop gain was redistributed to G_1. The resulting simulation is shown in Figure 6.13. The performance has improved greatly over that of figure 6.12, but the benefit of the integrator is only barely visible.

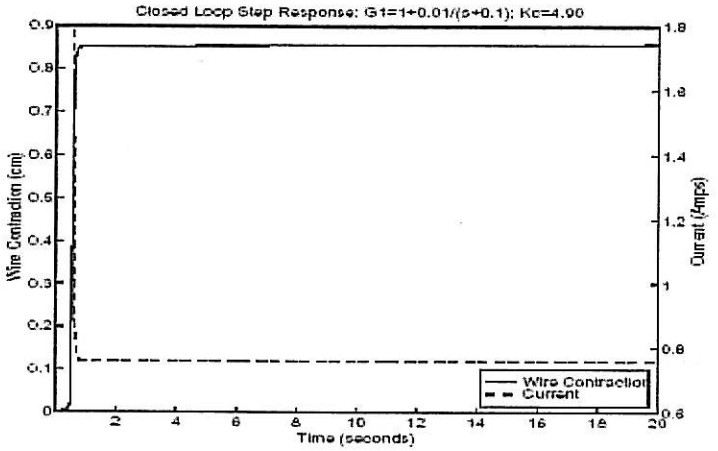

Figure 6.13 Closed Loop Step Response With $G_1 = 1 + \frac{0.01}{s + 0.1}$

CHAPTER 7

CONCLUSION & FUTURE WORKS

This chapter gives an overall conclusion for the project and also discusses some suggestions and ideas for the future development of this project.

7.1 Conclusions

As a conclusion, the overall objectives of this project have been achieved. The experimental system has been successfully developed using a single SMA wire actuator, under constant load. The result for a broad class of dissipative controllers when was applied to a simple SMA-actuated position control system, the system would be L2 stable for some range of non-zero loop gains. This applies to the common P, PI, PD and PID controllers, among others, and is believed to be first result of its kind. Beside that, the knowledge about shape memory alloys and shape memory actuator has been achieved due to excellent. The method to design SMA wire actuator was explained in this project.

It's also helps giving some guidance for development the SMA element as an actuator. Furthermore, methods were presented to determine the maximum stabilizing loop gain for a given controller and it is hoped that this project will become a platform for other students who are doing projects related to shape memory alloys.

7.2 Recommendations

Many avenues of future research have been uncovered during this work. To further improve this project, the author to suggest a few recommendations. First, for a stability of future research involves combining G_1 and G_2 to form one block, allowing the stability conditions for the two-block case to be applied. Due to the dimension and complexity of the function, graphical technique were insufficient to categories determine the range of stability. Another recommendation, this project also have been developed use the temperature sensor such like thermocouple or others to make measurement temperature of shape memory element and looks into the temperature-current relationship. The SMA actuators also were developed with two-wire actuator.

REFERENCES

1. Ramakant A. Gayakward (2000). " Op-Amp and Linear Integrated Circuit." Fourth Edition. New Jersey: Columbus, Ohio.

2. Robert Benjamin Gorbet (1996). " A Study of the Stability and Design of Shape Memory Alloy Actuators." Master's thesis, Univ. Waterloo. Ontario, Canada.

3. Tom Waram (1993). "Actuator Design Using Shape Memory Alloys." Hamilton, Ontario, Canada.

4. George B. Rutkowski, P.E.(1975). "Handbook of Integrated-Circuit Operational Amplifiers." Cleveland, Ohio.

5. Daniel R. Madill, David Wang, "Modeling and L2-stability of a Shape Memory Alloy Position Control System," in Proc. 1998 trans. on control systems technology., pp. 473-781.

6. Darel E. Hodgson, Shape Memory Applications Inc., Ming H. Wu, Memry Technologies,and Robert J. Biermann, Harrison. *Shape memory alloys, 1999,* http://www.sma-inc.com/SMAPaper.html

7. Shape Memory Alloy -inc, www.sma-inc.com

8. TiNi Alloy Company, http://www.sma-mems.com

9. www.ntu.edu.sg/mpe/research/researchnews

10. http://www.resonancepub.com/actuator.htm

11. www.araa.asn.au/acra/acra2002

GLOSSARY

A_f Temperature

Temperature at which the transformation from martensite to austenite is complete on heating.

A_S Temperature

The temperature at which austenite begins to form from martensite, on heating.

Austenite

General term for the high temperature phase of shape memory alloys; also referred to as the "parent" phase.

Beta (a) phase

The high temperature phase in copper-based alloys.

Biasing force

The force required to return a shape memory actuator to its low temperature position. This force can be supplied by gravity, a magnetic field, fluid pressure, or by a biasing mechanism such as a steel spring.

Bimetal

A composite material made of two interfacing strips of metals which have very different coefficients of thermal expansion. This results in the change in curvature of the bimetallic element in response to a temperature change.

Constrained Recovery

The partial recovery of strain (imposed at low temperature) obtained by heating a physically constrained shape memory element above the A_g temperature. This results in the generation of internal stress in the shape memory material.

Crystal Lattice Structure

An imaginary three dimensional array which describes the positions into which the atoms of a material arrange themselves under given conditions of stress, strain, and temperature.

Detwinning

The process in which all the martensite twin variants in a shape memory alloy align themselves in only one direction, as the result of an applied stress.

Extension Spring (shape memory)

A spring which contracts when heated, and is expanded at low temperature.

Fatigue

The physical failure of a metal (i.e. breakage} as the result of the application of a cyclic stress.

Free Length

The length to which a helical shape memory spring is shape set.

Free Recovery

The recovery of the hig h temperature shape of a shape memory element, under no imposed stress.

Heat of Transformation

The thermal energy released to, or taken from the environment which accompanies a phase transformation.

Hysteresis

Thermal - The temperature "loop" created by the difference exhibited in the transformation temperatures upon heating and cooling.
Mechanical - The difference between the upper and lower plateau stresses for a superelastic material, at a given temperature.

Martensite

In shape memory alloys, a low temperature twinned phase characterized by the ability to undergo detwinning at relatively low stress levels.

M_d Temperature

The temperature above which stress-induced martensite can no longer form, and all inelastic deformation is due to plastic deformation (slip).

M_f Temperature

Temperature at which the transformation to martensite is complete, on cooling.

Ms Temperature

Temperature at which martensite begins to form, on cooling.

One-Way Effect

The ability of a shape memory element to spontaneously recover a strain (i.e., or shape change) only during heating from low to high temperature; cooling from the high temperature state to low temperature does not result in any spontaneous macroscopic shape changes in the element.

Phase

A state of matter characterized by a unique physical or crystalline structure

Resistivity

A physical constant, unique to a material, which describes the opposition to the flow of an electric current.

Shape Memory Effect

The ability of an alloy to undergo a thermally reversible change of shape (i.e., strain recovery), due to a change in crystal structure.

Superelasticity

The ability of an alloy to accumulate large amounts of reversible strain due to the formation of stress-induced martensite above the A_f temperature and below the M_d temperature; the strain is recovered when the applied stress is released.

Twinning (mechanical)

A microscopic deformation mechanism in metals in which adjacent areas of the crystal lattice acquire orientations which are mirror images of one another, through a plane of symmetry. In shape memory alloys, the energy required for twin formation is relatively small.

Two-Way Effect

The ability of a shape memory element to recover all or part of its low temperature shape (i.e., or strain) upon cooling, in addition to the "normal" ability to attain its separate, high temperature shape on heating.

Work Production

The conversion of thermal energy to mechanical energy by a shape memory element. A simple example is a shape memory wire which lifts a weight when heated.

Yield Strength

The stress level at which non-elastic deformation begins to occur in a shape memory alloy. In general this deformation can be caused by either slip, or by the formation of stress-induced martensite.

Young's Modulus

The slope of the uniaxial stress-strain curve in its linear-elastic portion. The Young's modulus of shape memory alloys is very dependent on temperature.

APPENDIX A

PICTURES OF PROJECT

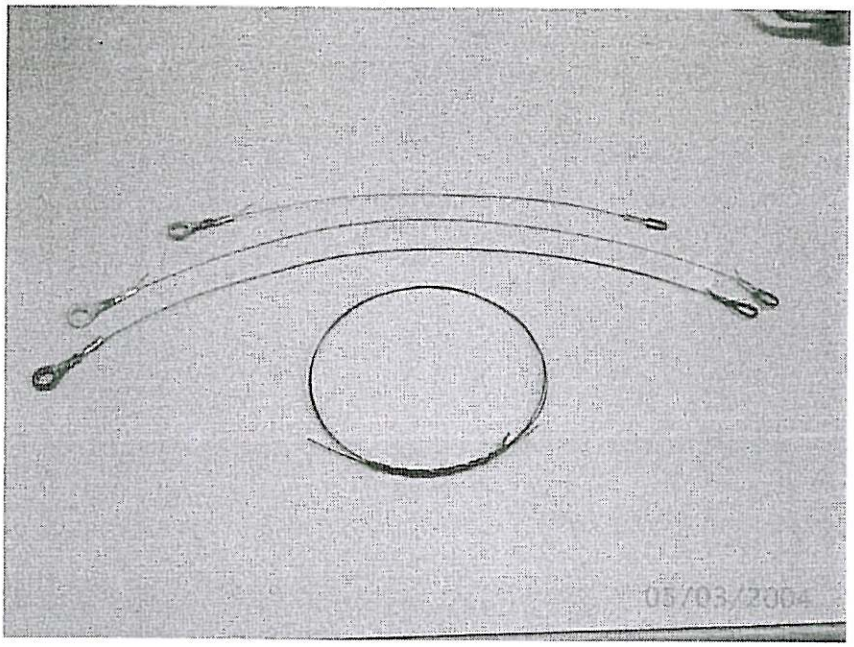

Picture 1 Shape Memory Alloy wire

Picture 2 Experimental system

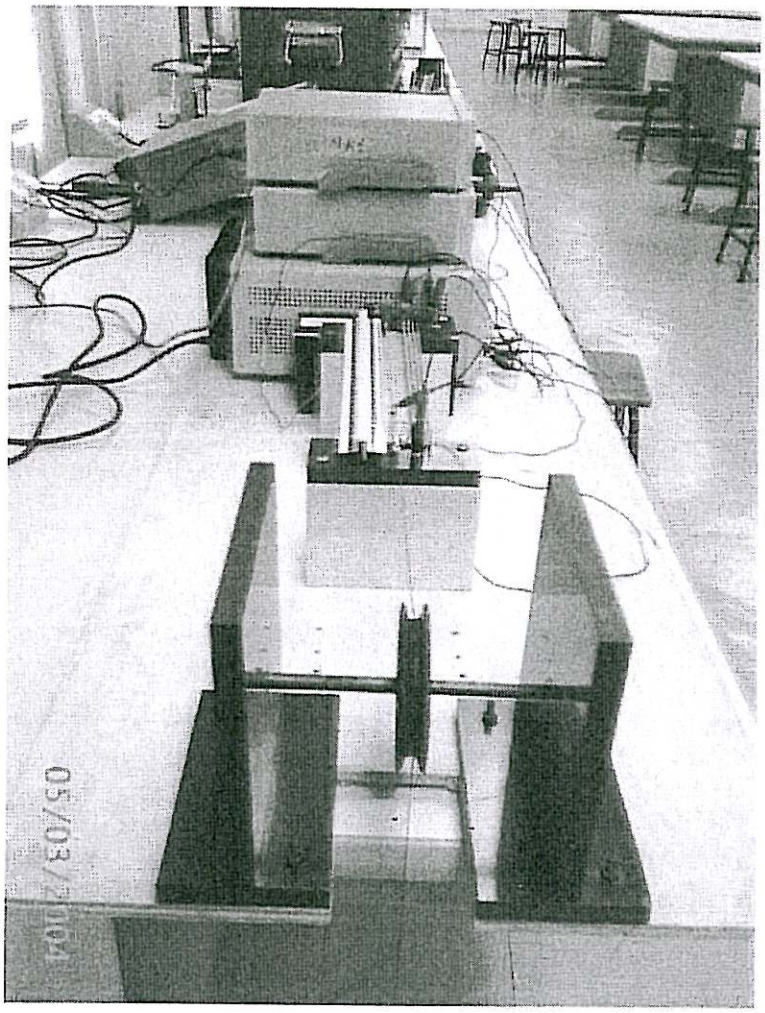

Picture 3 View side of project

APPENDIX B

DATASHEETS MATERIAL OF PROJECT

Acetal pulleys

Acetal bearings and wheels with stainless steel balls. The excellent mechanical properties of acetal resins include fatigue resistance, low friction and wear, high stiffness, strength and hardness plus good dimensional stability.
Applications include belt-conveyor rollers, dairy machinery, filing cabinets, floppy-disc drives, photocopiers, photographic processing equipment, robotics and weighing machines.

- Chemical and corrosion resistant
- Light weight
- Low friction
- Flexibility of design and manufacture

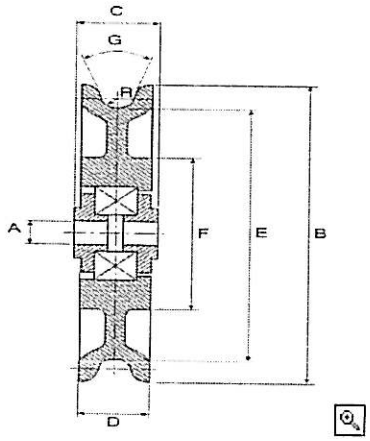

Two sizes of acetal pulleys containing carbon steel ball bearings.

A	B	C	D	E	F	G°	R	kg
9·5	102 (4in.)	20	18	83·3	58	30	4	200
9·5	152 (6in.)	20	18	134·1	58	30	4	200

Torlon rod

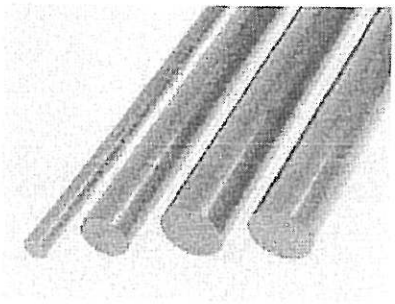

Provides better compressive strength and higher impact resistance than most high performance plastics. Extremely low coefficient of thermal expansion and high creep resistance. It also offers good chemical and radiation resistance.
Environmental: Torlon is unaffected by strong acid (pH□3). Ultra violet light and strong alkali will cause dimensional change. Steam at 160°C will cause decomposition.
Similar to the electrical grade, but modified with the addition of graphite and fluorocarbon for good wear resistance, low friction and high compressive strength.
Applications include bearings, thrust washers, wear pads, and piston rings.
Colour: green/black.

physical properties

Specific gravity	1·45
Tensile strength (23°C dry)	164 N/mm^2
Elongation (23°C dry)	7·0%
Tensile modulus (23°C dry)	6,600 N/mm^2
Flexural strength (23°C dry)	219 N/mm^2
Flexural modulus (23°C dry)	6900 N/mm^2
Hardness (Rockwell)	E72
Coeff. of linear thermal expansion	$2{\cdot}52K^{-1}x10^{-5}$
Coeff. of thermal conductivity	0·54W/K.m
Max. long term service temp.	+230°C

Min. long term service temp.	-195°C
UL flammability	V-O (1·17)
Coeff. of friction:	
-dry against steel -dynamic	0·13-0·17

Tufnol

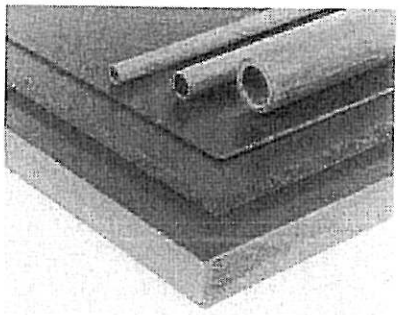

Kite is the most widely used of all TUFNOL grades where ever a first class quality electrical insulation material is required for low, medium or high voltages. It has good dielectric strength and high insulation resistance with low moisture absorption and good mechanical strength. Kite Brand meets BS2572 Type P3 (EN60893 type PF CP 206) equivalent to the former BS5102 Type 1 and BS1137 Type 1, which have been widely used in the electrical industry for many years. It is readily machinable and can be hot punched in thickness up to 3·2mm.
Applications include terminal boards, mounting panels, tag strips, coil formers, insulating sleeves and bushes, busbar supports,coil supports, insulated enclosures, brush holders, insulating spacers, plugs and sockets.

technical specification

Cross break. str.		175	MPa
Impact strength, notched, charpy		2·7	kJ/m^2
Compressive strength, flatwise		350	MPa
Compressive strength, edgewise		200	MPa
Resistance to flatwise comp.		1·2	%
Shear str. flatwise		105	MPa
Water absorb:	1·6mm thk	39	mg
	6·0mm thk	56	mg
	12·0mm thk	70	mg
Electric strength:			
Flatwise in oil at 90°C:			
	1·6mm thk	14·5	MV/m

	6·0mm thk	8·8	MV/m
	12·0mm thk	8·1	MV/m
Edgewise in oil at 90°C		55·0	kV
Insulation resistance after immersion in water:			
		$1x10^9$	ohms
Loss tang. at 1MHz		0·037	
Perm. at 1MHz		5·1	
Relative density		1·36	
Max. working temperatures:			
	cont.	90°C	
	interm.	120°C	
Suggested thermal classification - Class E			
Thermal cond. through laminal		0·26	W/(mK)
Thermal expansion in plane of laminal		1·8	x10
Specific heat		1·5	kJ/(kgK)